TECHNICAL UNIVERSITY OF LIBEREC
Faculty of Mechatronics, Informatics
and Interdisciplinary Studies

Synthesis of pyrrole-cyclodextrin conjugates for tissue engineering

Ph.D. thesis - short summary

Study program: P3901 – Applied Sciences in Engineering
Field of study: 3901V055 – Applied Sciences in Engineering

Author: **Ing. Jan Lukášek**
Supervisor: prof. Ing. Ivan Stibor, CSc.

Liberec 2019

TECHNICKÁ UNIVERZITA V LIBERCI
Fakulta mechatroniky, informatiky
a mezioborových studií

Syntéza pyrrol-cyklodextrinových konjugátů pro tkáňové inženýrství

Disertační práce - krátké shrnutí

Studijní program: P3901 – Aplikované vědy v inženýrství
Studijní obor: 3901V055 – Aplikované vědy v inženýrství

Autor práce: **Ing. Jan Lukášek**
vedoucí práce: prof. Ing. Ivan Stibor, CSc.

Liberec 2019

Declaration

I hereby certify that I have been informed that Act 121/2000, the Copyright Act of the Czech Republic, namely Section 60, School-work, applies to my dissertation in full scope. I acknowledge that the Technical University of Liberec (TUL) does not infringe my copyrights by using my dissertation for TUL's internal purposes.

I am aware of my obligation to inform TUL on having used or licensed to use my dissertation in which event TUL may require compensation of costs incurred in creating the work at up to their actual amount.

I have written my dissertation myself using literature listed therein and consulting it with my supervisor.

I hereby also declare that the hard copy of my dissertation is identical with its electronics form as saved at the IS STAG portal.

Date:

Signature:

ACKNOWLEDGEMENT

In the first place I would like to thank my wife and family for supporting me throughout writing this thesis and the whole studies.

I am also grateful to prof. Ivan Stibor for his professional leadership and kind attitude. I appreciated his extensive knowledge and experience, which helped me to overcome numerous obstacles I have been facing throughout my research. I could not have imagined having a better advisor and mentor for my Ph.D. study.

I would like to thank all, who assisted me with characterisation of prepared compounds or materials. Namely, to Dr. Markéta Řezanková for measuring NMR spectra, Dr. Pavel Kejzlar for SEM characterisation, Ing. Martin Stuchlík and also to Dr. Jana Müllerová for providing thermogravimetric and IR analysis together with evaluation of the obtained data.

In addition, my sincere thanks go to colleagues from the Department of Nonwovens and Nanofibrous Materials for their cooperation on the project, delivering fibrous samples and the extensive *in-vitro* experiments.

Nevertheless, I would like to express my gratitude to Dr. Michal Řezanka and fellow colleagues from our laboratory for their friendship and creating a pleasant atmosphere during the years spent at Technical University of Liberec.

TARGETS OF THIS WORK

This thesis aims to prepare new composite material for tissue engineering and to understand the effect of surface functionalization on the cell-material interaction. This scaffold will serve as a primary platform for future development towards its ultimate application in the field of nervous tissue regeneration. Despite decades of intensive research, the majority of implants suffers from many drawbacks. One of them is the inertness of material which cannot provide essential cues for cell stimulation and growth. However, contemporary analytical chemistry together with advanced techniques for materials synthesis offers considerable variability in scaffolds design. Therefore, we have decided to combine knowledge from several different research areas and create procedures for the preparation of novel materials with exciting features. Our scaffold is based on the 3D fibrous polymeric network made by electrospinning process. This technique enables the production of materials with tunable mechanical properties, morphology or stability in the physiological environment. Although electrospinning is a random process, there is reasonable control over the diameter and morphology of the fibres. Other indisputable advantages are high productivity and the possibility of incorporating various compounds, nanoparticles or even biomolecules into the fibrous structure. Moreover, aligned fibres can also be prepared using a rotating collector or by drawing technique which is under intensive development in cooperation with our colleagues. The orientation of fibres also imparts another level of control over the cell adhesion and growth.

It is generally known that adhesive proteins mediate cell-material interaction. These biomolecules are absorbed onto the surface and are recognised by specific membrane receptors. Therefore, one option of our research is the synthesis of pyrrole-cyclodextrin monomers which could be copolymerized with pyrrole creating desirable core-shell material with cyclodextrin decorated surface. The alternative route would be based on the preparation of a fibrous matrix with deposited β-substituted polypyrrole layer. In the next step, suitable binding places would be utilised for the final cyclodextrin immobilisation. We believe, that cyclodextrin lipophilic cavity could attract adhesion-mediating proteins by non-bonding interaction and thus create extracellular matrix mimicking structures on the surface. Such interactions allow absorption of proteins in their natural spatial conformation which ultimately leads to significantly better cell adhesion and growth. Moreover, the core-shell 3D matrix with a deposited conductive polypyrrole layer on the surface could be used for cell guidance by external electric stimulation. The study of the scaffold mentioned above should bring us new information about cell-material interaction and make a step forward to the future bioresponsive material for tissue engineering.

Keywords: pyrrole, cyclodextrin, polypyrrole, surface functionalization, tissue engineering

CÍLE PRÁCE

Tato práce si klade za cíl připravit pokročilý materiál pro tkáňové inženýrství a především hlouběji pochopit vliv povrchové úpravy na interakci substrátu s biologickou hmotou. Tento materiál dále poslouží jako platforma pro cílovou aplikaci v oblasti regenerace nervové tkáně. Navzdory intenzivnímu výzkumu v průběhu posledních několika dekád trpí tkáňové nosiče řadou nedostatků. Jedním z nich je netečnost implantátů, které neposkytují nezbytné podněty pro stimulaci buněčného růstu. Současná analytická chemie však disponuje širokou paletou metod, které nám pomáhají pochopit základní děje probíhající při interakci biologické hmoty s povrchem materiálu. Tyto nástroje také hrají důležitou roli při designování nových tkáňových nosičů, které dnes mohou být připraveny řadou pokročilých metod. Nejen proto jsme se rozhodli zkombinovat znalosti z několika různých oblastí a vytvořit postup pro přípravu pokročilého materiálu se zajímavými vlastnostmi pro tkáňové inženýrství. Námi navržený tkáňový nosič je postaven na 3D vlákenné polymerní síti, která byla vyrobena elektrostatickým zvlákňováním. Tato technika umožňuje produkci vlákenného materiálu s variabilními mechanickými vlastnostmi, morfologií nebo stabilitou ve fyziologickém prostředí. Ačkoliv elektrostatické zvlákňování produkuje náhodně uspořádaná vlákna, tak poskytuje dobrou kontrolu nad průměrem vláken či tloušťkou vznikající vrstvy. Orientace vláken dále propůjčuje materiálu schopnost ovlivňovat směr růstu buněk.

Je obecně známo, že interakce většiny typů buněk s materiálem je zprostředkována adhezními proteiny. Tyto biomolekuly jsou adsorbovány na povrchu a následně rozpoznány specifickými membránovými receptory. Záměrem našeho výzkumu je v první řadě syntéza pyrrol-cyklodextrinových derivátů, které mohou být následně deponovány na povrch zvoleného materiálu. Alternativní cestou je pokrytí vlákenného substrátu vhodným β-substituovaným derivátem polypyrrolu, jehož funkční skupiny budou v následném kroku využity pro navázání cyklodextrinových makrocyklů. Věříme, že lipofilní kavita cyklodextrinu umožní díky slabým nevazebným interakcím s proteiny jejich přitažení k povrchu, čímž dojde k vytvoření struktury připomínající extracelulární hmotu. Tato interakce povede k adsorpci proteinů v jejich přirozené prostorové konformaci, což bude mít za následek lepší adhezi a proliferaci buněk. Povrchová vrstva vodivého polypyrrolu může být navíc využita k elektrické stimulaci růstu buněk. Očekáváme, že studium takového tkáňového nosiče přinese zajímavé informace o interakci buněk s materiálem a otevře cestu k pokročilým biologicky aktivním materiálům pro tkáňové inženýrství.

Keywords: pyrrol, cyklodextrin, polypyrrol, funkcionalizace povrchu, tkáňové inženýrství

CONTENT

1. INTRODUCTION

Although thousands of different materials for tissue engineering have been prepared over the last years, human creations are still not precise nor useful as the creations of nature. On the other hand, the understanding of biological processes gone through tremendous development which help us to design tailor-made materials with tunable properties according to a target application. That is why we decided to create new composite material and contribute to a better understanding of cell-material interaction. The work is divided into several follow-up steps, starting with the synthesis of suitable pyrrole derivatives. Then, these compounds will be polymerised onto the 3D matrix, and the structure of resulting core-shell fibrous material will be characterised by analytical methods. There are two possible scenarios for the final cyclodextrin immobilisation. The pyrrole monomer could be directly connected to cyclodextrin and then *in-situ* copolymerized with pyrrole in order to prepare desirable coated material. Alternatively, the fibrous scaffold could be covered with polypyrrole derivative before the cyclodextrin attachment using one of many available conjugation techniques (Figure 1). The effects of surface functionalization and the biocompatibility will be later studied by *in-vitro* experiments.

The theoretical part would provide a reader with brief information about pyrrole derivatisation, conductive polymers and mechanisms of cell-material interaction. Results and discussions represent the core chapter where measured data are critically evaluated. The experimental part describes the exact procedures for the synthesis of pyrrole derivatives with the corresponding spectroscopic analysis. The final section deals with the polypyrrole deposition, cyclodextrin immobilisation, material characterisation and *in-vitro* study.

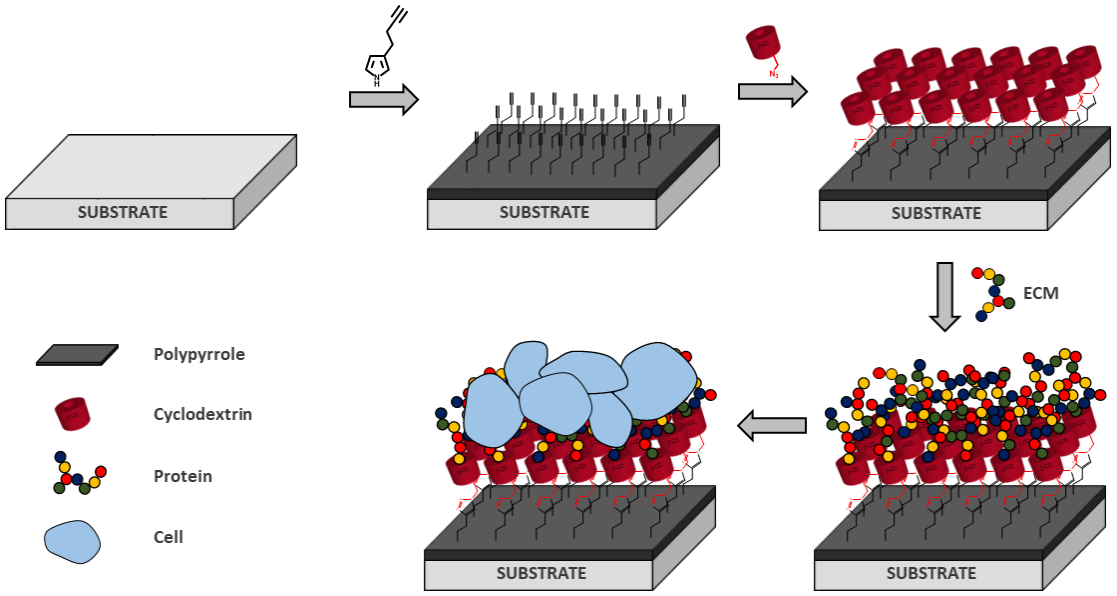

Figure 1. Preparation of PPy-CD material for tissue engineering

2. THEORETICAL PART

2.1. Pyrrole – synthesis and reactivity

Pyrrole is a five-membered heterocycle like furan and thiophene. It is a colourless liquid that darkens upon exposure to air. Unsubstituted pyrrole is produced industrially by treatment of furan with ammonia in the presence of a catalyst. In laboratory scale, it is synthesised by Hantzsch[1], Knorr[2] or Paal-Knorr[3] reaction. Many alkaloids or drugs containing pyrrole heterocycle unit can be directly prepared by multicomponent reactions.[4] Natural products like porphyrins, indoles, bilirubin or vitamin B12 contain pyrrole in their structure as well.[5,6]

Pyrrole is less basic than pyridine due to the conjugation of nitrogen lone electron pair into the aromatic ring. It can be derivatised at the nitrogen or carbon atoms (Scheme 1). Protonation by strong acids occurs mainly (80 %) at C2 and partially (20 %) at the nitrogen atom. Reactions with electrophiles yield 2-substituted pyrroles because of higher electron density at C2 compared to position C3.

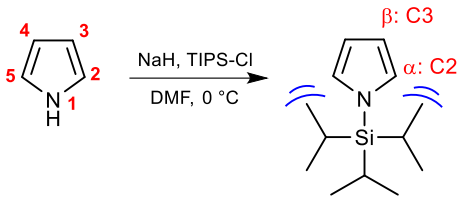

Scheme 1. Structure and numbering of pyrrole

Polysubstituted derivatives can be easily prepared if an excess of the electrophilic agent is used. Halogenation, nitration, sulfonation are well-established methods providing mono-, di-, tri- or tetra- substituted pyrroles with different selectivity.[7–10] Mono-substitution at position C3 is not directly accessible, but various approaches can be used for selective derivatization.[11–13]

1. Introduction of acyl group at C2, which directs substitution to C3 and can be selectively removed after the reaction
2. The acid-catalysed isomerisation of C2 derivatives
3. Blocking of C2 position with bulky *N*-protecting group

The most convenient way for β-substitution is method 3. The nitrogen can be protected with sulfonyl or silyl group which hinder more reactive α–positions, and therefore subsequent electrophilic aromatic substitution affords β–derivatives preferably. Then, protecting group is easily cleaved to yield pyrrole exclusively substituted at position C3.[8,10,14]

2.2. Conductive polymers

2.2.1. Historical milestones

An enormous effort has been made to study and utilise conductive polymers during the last four decades. They are often called “synthetic metals” because of their intrinsic conductivity which is normally associated only with the metals.[15]

The first conductive polymer was probably prepared in 1874 from aniline by treatment with sulphuric acid which resulted in black powder polyaniline. Later, highly explosive sulphur nitride was found to be superconductive at extremely low temperature (T_c = 0.24 K).[16] In 1974 Shirakawa has developed a procedure for the synthesis of *cis* or *trans* polyacetylene by Ziegler Natta catalyst.[17] Despite the crystalline metallic structure, the resulting polyacetylene film was air sensitive insulator. However, just three years later in 1977, an article dealing with the synthesis of the first truly conductive polymer was published.[18] Shirakawa and his co-workers observed a drastic change in infrared absorption of polyacetylene treated with halogen vapours. Joint efforts of two American physicists Alan J. Heeger, Alan G. MacDiarmid and Shirakawa´s team resulted in the discovery of first truly conductive polymer. The series of experiments revealed that conductivity was increased by order 10^9 because of “doping”. Their work opened the way for further study of conductive polymers and was greatly rewarded with the Nobel Prize for Chemistry in 2000.[19] Scientific community quickly realised the potential of this new brand of compounds and several other conductive polymers were synthesised during upcoming years (Figure 2). The most prominent examples were polyaniline, polythiophene, polypyrrole and their derivatives. Such polymers found many applications in electronics, light emitting diodes, flat screen, sensors, supercapacitors or later in tissue engineering.[20–24]

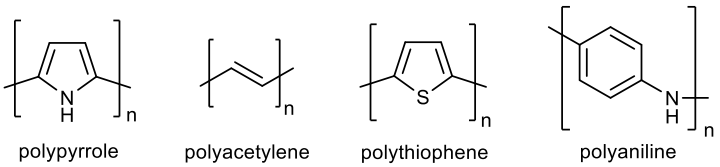

polypyrrole polyacetylene polythiophene polyaniline

Figure 2. Structures of common conjugated polymers

2.3. Cell-material interaction

Thousands of promising materials for tissue engineering have been made over the last years. Inorganic, as well as organic materials, found their place in modern medicine, but an ideal material for replacing damaged tissue has not been found yet. Chemical and physical properties of bulk material are well understood and can be tailored according to the desired application. The surface topography and morphology are the next things to consider before designing a new scaffold. Cells can sense different surface roughness even at nanometer level which can cause apoptosis in the worst case. An overall cellular-surface response may be understood as biocompatibility.[25] Such a material improves biological functions, adhesion and growth of cells while it does not cause an inflammatory reaction. These interactions can be explained in a very simplified manner as follows. First, the surface is covered by ECM proteins to form a dynamic equilibrium. Then, cells bind to adhered proteins *via* specific membrane proteins called integrins. After initial interaction, cells begin to secrete their own proteins and communicate with other cells by one of many signalling pathways. The result is the gene expression followed by cell replication on the protein covered surface (Figure 3).

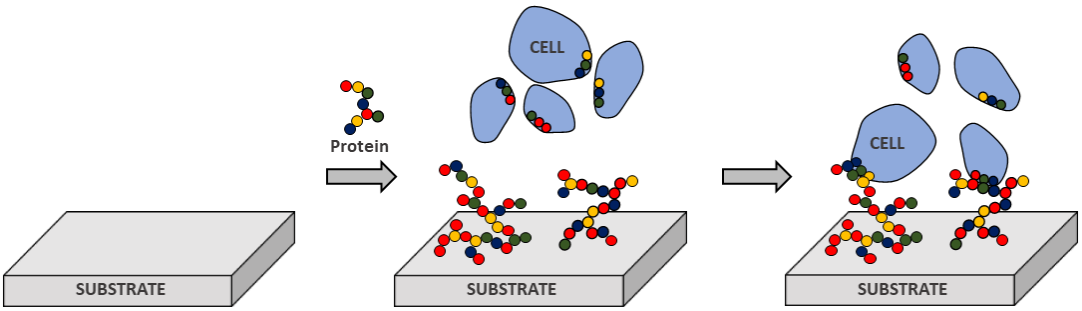

Figure 3. Cell-substrate interaction *via* integrin receptors

3. RESULTS AND DISCUSSION

3.1. Retrosynthesis of target compounds

The retrosynthetic approach leading to the target conjugates is described below (Scheme 2). We can start the retrosynthetic analysis of compound **A** with C-N bond disconnection. All mono substituted cyclodextrins **C**, **D** and **E** are easily accessible and can be synthesized from commercially available β−cyclodextrin **F**. Further, molecule **B** with tuneable carbon linker length can be prepared by extension of procedure published by Stefan et al.[112] First, pyrrole **J** is protected at nitrogen with bulky group and then compound **I** is selectively mono-brominated at position C3. Alkylation of compound **H** yields molecule **G** which is subsequently transformed into **B** using metal-halogen exchange reaction. The final conjugation between amino cyclodextrin **C** and activated ester of molecule **B** gives target molecule **A**. In the case of molecule **K**, a double C-N disconnection provides synthon **L** and the azido cyclodextrin **D** as was described before. Molecule **L** can be directly prepared from **G** by S_N2 substitution of halogen with acetylide anion. Conjugation of **K** and **L** is then carried out by CuAAC as a final synthetic step.

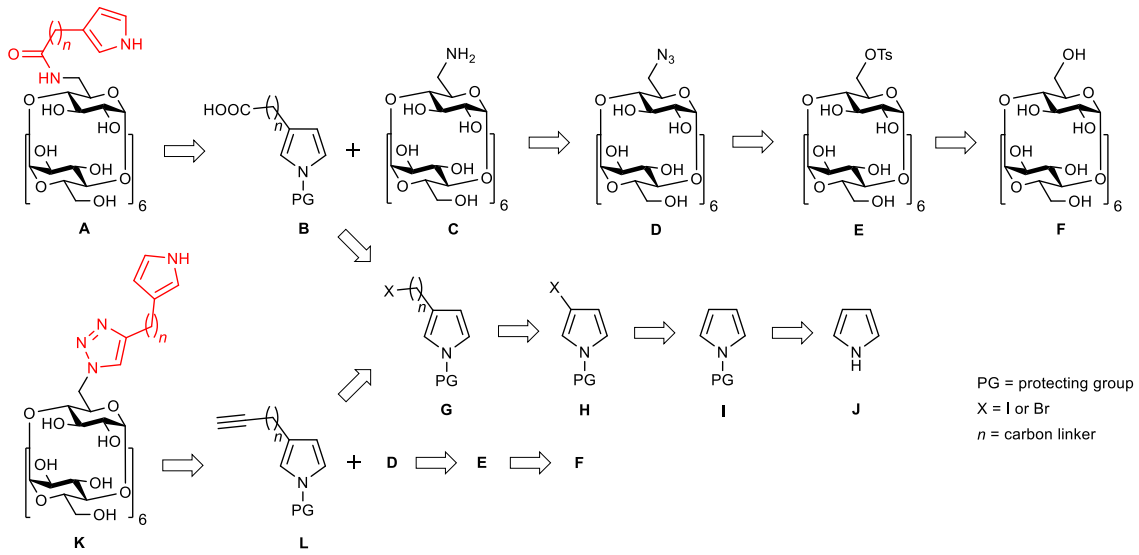

Scheme 2. Retrosynthetic analysis of target pyrrole-cyclodextrin conjugates

3.2. Synthesis of pyrroles for CD conjugation

3.2.1. Substitution of pyrrole at β–position

As was previously mentioned in the first part of the thesis, the β–substituted derivatives are not directly accessible by electrophilic aromatic substitution. Thus, pyrrole **1** was firstly protected at nitrogen with bulky TIPS group to enhance the selectivity of the next reaction step (Scheme 3). Treatment of pyrrole **1** with 1.1 eq. of sodium hydride in dry DMF at 0 °C for 2 hours under argon afforded product **2** in 68% yield after final vacuum distillation. This product is also available commercially. The selective derivatisation of compound **2** at the β–position was carried out in THF at -78 °C using 1.05 eq. of NBS as a brominating agent. After purification by vacuum distillation, the product **3** was obtained in 81% yield together with 5 % of α–isomer **4**.[10] It is generally known that bromo compounds are less reactive in Pd-catalysed cross-coupling reactions. Therefore, the corresponding iodo pyrrole derivative **5** was prepared by halogenation of **2** with 1 eq. of NIS at low temperature in excellent yield as well.[8]

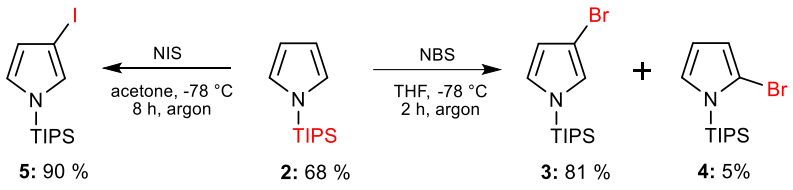

Scheme 3. Synthesis of mono halogenated pyrrole derivatives

Halogen substituted derivatives **3** or **5** were alkylated by 1,5-diiodopentane and 1,10-diiododecane. The starting compound was subjected to metal-halogen exchange reaction with *n*-BuLi in THF at room temperature and the *in situ* generated lithium intermediate was reacted with an excess of the alkylating agent (Scheme 4). Products **6** and **7** were isolated after column chromatography on silica gel in 67% and 43% yield respectively.

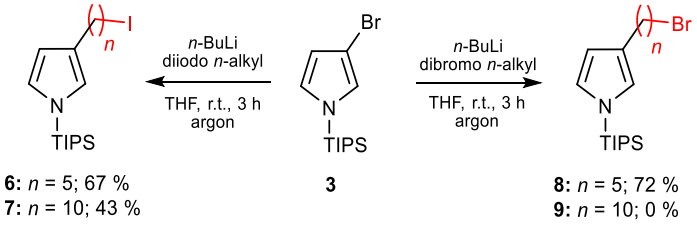

Scheme 4. Alkylation of β–substituted pyrrole **3**

Both new compounds were characterised by HRMS, 1D and 2D NMR spectroscopy. Three signals of corresponding hydrogen atoms in aromatic part of the ^{1}H NMR spectrum suggested the monosubstitution of the pyrrole ring. The rest of the signals were assigned to alkyl

chain with terminal iodine and the nitrogen protecting TIPS group. Combined information obtained from COSY, HSQC and HMBC spectra confirmed the structure of compounds **6** and **7**.

Because the 1,5-dibromopentane is roughly 15 times cheaper than the corresponding iodo compound, it can be used instead. Another benefit is that the excess of 1,5-dibromopentane can be easily distilled off after the reaction. Hence, the chromatography of crude product is more straightforward, and the unreacted alkylation agent can be recovered. The compound **8** was prepared in good yield, but low reactivity of 1,10-dibromodecane against lithiated intermediate was found despite the published literature.[26] Only a trace amount of product **9** was formed even when the reaction time was prolonged from 3 to 24 hours. Thus, a cheaper 1,5-dibromopentane was used for the synthesis of derivatives with five carbon linker, and the more reactive 1,10-diiododecane was used as an alkylating agent for the synthesis of derivatives with a longer linker.

3.2.2. Synthesis of pyrroles with the carboxylic group

Treatment of **3** with *n*-BuLi followed by addition of dry ice afforded pure compound **10** in 88% yield after recrystallization from EtAc (Scheme 5).[10] Pyrrole-carboxylic acids **11** and **12** were synthesized by modified procedure published by Stefan et. al.[26] First, we took over their original protocol, where **8** was transformed into Grignard reagent and reacted with excess of CO_2. However, the reaction of Mg pellets catalysed with I_2 in dry etheric solvent failed. Thus, *t*-BuLi was used to generate reactive nucleophilic species at - 78 °C in THF and after that dry CO_2 was bubbled through the solution. Acidic workup afforded crude reaction product which was purified by column chromatography on silica gel with gradient elution. Pyrrole-carboxylic acids **11** and **12** were isolated in 64% and 51% yield respectively.

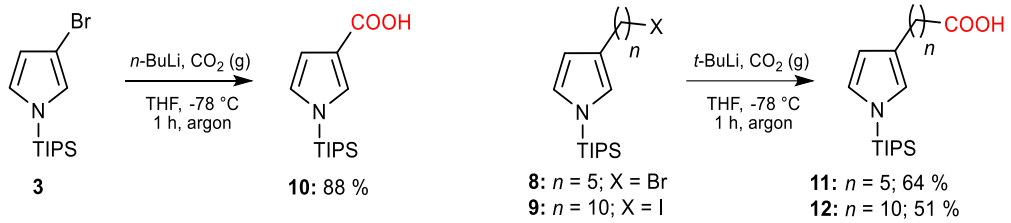

Scheme 5. Synthesis of pyrrole carboxylic acids

3.2.3. Synthesis of pyrroles with a triple bond

Despite the simplicity of the pyrrole structure only a few examples of triple bond substituted derivatives are published. It may be caused by instability of some molecules with a free terminal triple bond or unnecessary use of these compounds before the CuAAC reaction rediscovery.[27-29] Therefore, a new synthetic route for the synthesis of a triple bond substituted pyrroles with tuneable carbon linker length (0, 4 or 9 carbons) has been developed (Scheme 6).

First, the synthesis of pyrrole **15** with directly connected triple bond was examined. Starting from iodo derivative **5** the compound **13** was prepared using the Pd-catalysed Sonogashira cross-coupling reaction in 66% yield.[8,30] It was reported that deprotection of this compound with 1 eq. of TBAF provides unstable product **14** which spontaneously decomposes. Thus, selective deprotection of the TMS group by K_2CO_3 in MeOH at room temperature was carried out to afford target molecule **15** in reasonable yield. Later, our synthetic protocol was improved, and compound **15** was synthesised directly from iodo pyrrole **5**. Coupling of compound **5** with ethynylmagnesium bromide under Kumada reaction conditions opened a straightforward way to the target molecule **15**.[31-33] A great advantage of this one-step procedure is high selectivity, mild reaction conditions and easy purification.

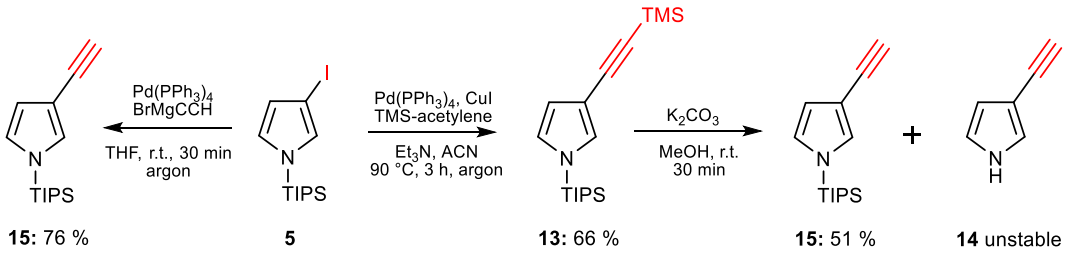

Scheme 6. Synthesis of TIPS-protected pyrroles with a directly connected triple bond

Further, the synthesis of pyrroles with triple bond on carbon linker was studied. Typically, molecules with the aliphatic triple bond are prepared by simple substitution of the corresponding I, Br, or Cl atom in the sense of nucleophilic substitution by acetylide anion. Surprisingly, the reaction of compound **6** or **7** with sodium acetylide, TMS-protected lithium acetylide, or lithium acetylide ethylenediamine complex in DMSO or THF afforded only a trace amount of desired product (Scheme 7).[34, 35] If the ethynylmagnesium bromide was used as a nucleophilic agent an unexpected product of halogen exchange **8** was isolated in 82% yield instead of the desired molecule.

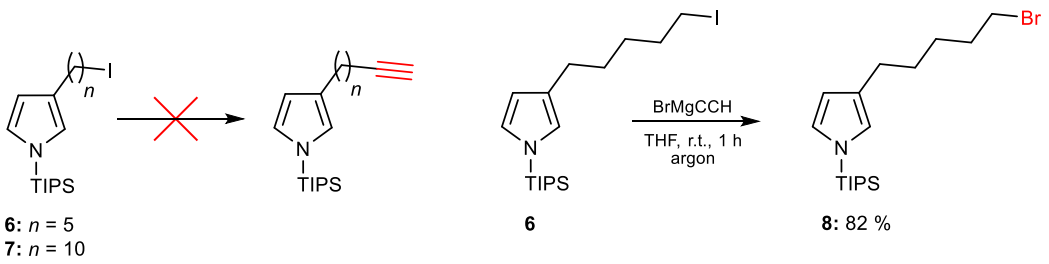

Scheme 7. Nucleophilic substitution of halogen atom with acetylide anion

Due to these unsuccessful attempts, another multistep synthetic procedure including Corey-Fuchs reaction[36] as a final transformation has been proposed (Scheme 8). The bromine atom was substituted with cyano group by reaction of **8** with NaCN in moderate yield. However, subsequent reduction of nitrile with DIBAH in toluene gave an only low yield of target aldehyde.[37,38] The key intermediate for the Corey-Fuchs reaction was finally prepared by Kornblum oxidation.[39] The reaction of pyrrole **6** or **7** with 2 eq. of $NaHCO_3$ in DMSO at 110 °C furnished crude products which were purified by column chromatography on silica gel. Aldehydes **16** and **17** were isolated in 71% and 58% yield respectively. The transformation of halogen to the carbonyl group was also carried out starting from bromopyrrole **8**, but the reaction must be further catalysed with 1.5 eq. of NaI.[40] Then, *in situ* generated iodo compound is converted into aldehyde **16**. It is interesting to mention that the Kornblum oxidation can be done in microwave reactor with high yields over 90 % as published by Bratulescu.[41] Next, geminal dibromo olefins **18** and **19** were prepared by reaction of aldehydes **16** or **17** with PPh_3, CBr_4 in DCM at 0 °C. The structure of these compounds was confirmed by NMR where the signal of the CHO group in ^{1}H NMR disappeared whereas triplet of vinyl hydrogen atom appeared around 6.40 ppm strongly influenced by two electron withdrawing bromine atoms. Finally, the triple bond substituted pyrroles **20** and **21** were prepared in almost quantitative yields by the elimination of bromines with 2 eq. of *n*-BuLi in THF at 0 °C.

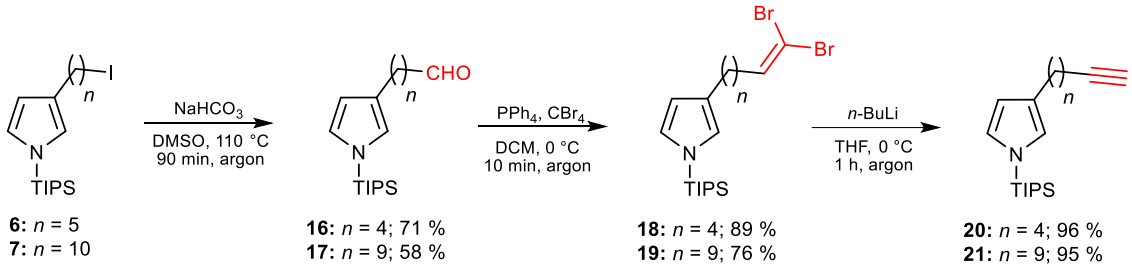

6: *n* = 5
7: *n* = 10

16: *n* = 4; 71 %
17: *n* = 9; 58 %

18: *n* = 4; 89 %
19: *n* = 9; 76 %

20: *n* = 4; 96 %
21: *n* = 9; 95 %

Scheme 8. Synthesis of pyrrole derivatives **20** and **21**

3.2.4. Deprotection of selected silylated pyrroles

Although many of β-substituted pyrrole derivatives without protecting group at the nitrogen atom are unstable, the possibility of TIPS cleavage from the compounds **10**, **11**, **12** and **15**, **20**, **21, 26** was examined.[8,10] The corresponding pyrroles could serve as essential intermediates on the way to tuneable polypyrrole coatings. While the pending carboxy group can be coupled with various biomolecules, e.g. growth factor or specific amino acid sequences *via* an amide bond, the multiple terminal bond offers even greater conjugation possibilities using one of many CLICK reactions. Is also generally agreed that *N*-substitution is lowering the polypyrrole conductivity

due to substantial planarity disruption compared to β-substituted derivatives. The silyl protecting group was removed from all seven compounds using 1.05 eq of TBAF as a source of fluoride anion, and the crude reaction products were purified by column chromatography (Scheme 9). Three acids **27**, **28** and **29** were obtained in high yields as solids without any stability issues at standard conditions. Same reaction procedure has been used for the synthesis of pyrroles with a terminal triple bond. However, the pyrrole **14** with directly connected triple bond was subject of immediate decomposition as reported by Alvarez[8] while derivatives **30** and **31** were easily isolated after column chromatography in good yields. The pyrrole derivative **32** with a terminal double bond was synthesised by the same procedure as well.

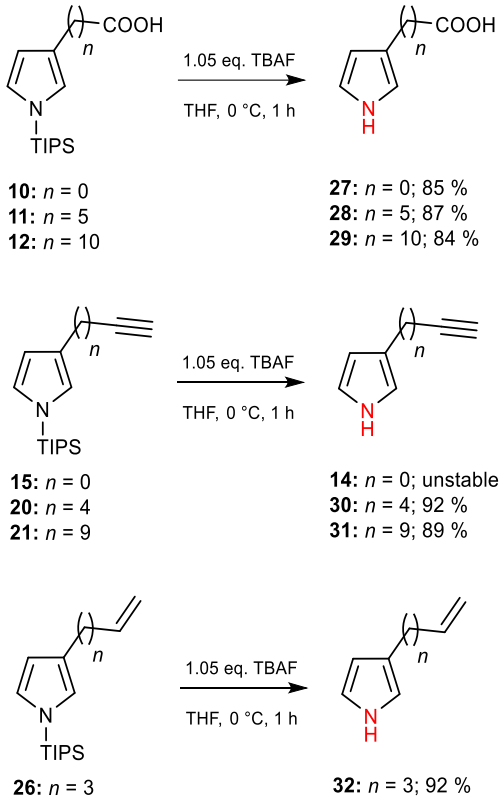

Scheme 9. The cleavage of silyl protecting group from the selected pyrroles

3.3. Synthesis of Py-CD monomers

Two strategies for pyrrole-cyclodextrin conjugation were studied. First, pyrrole carboxylic acids **10**, **11** and **12** were directly connected with 6^A-deoxy-6^A-amino-β-CD **36** using amide bond. Activation of the carboxy group with EDC/NHS ester has proven to be a practical approach but without needed selectivity. The activated ester reacted with NH_2 group but also with other hydroxyl groups on cyclodextrin macrocycle to form an inseparable mixture of isomers. Therefore, a more selective type of activation with PyBOP/DIPEA in DMF was tested (Scheme 10).[42] After the full conversion of starting compound, a mixture of HF/Et_3N was added to cleave TIPS protecting the group. The solution of TBAF was also used as a deprotecting agent, but purification was more complicated compared to the previous example. Three target molecules **45**, **46** and **47** with β-CD on different carbon linkers were successfully prepared in excellent yields without the need of chromatographic purification.

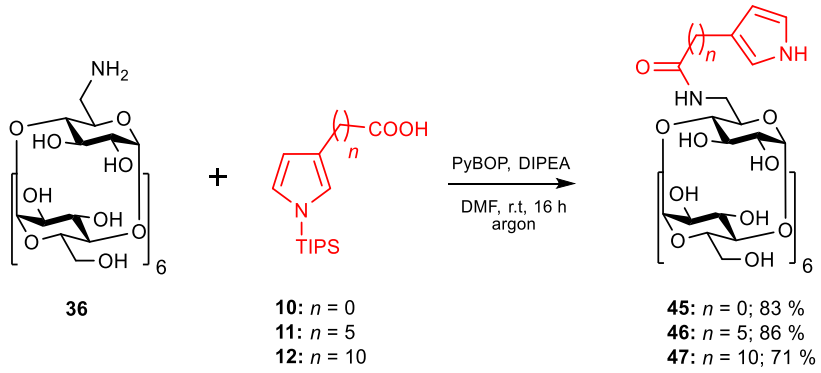

36

10: *n* = 0
11: *n* = 5
12: *n* = 10

45: *n* = 0; 83 %
46: *n* = 5; 86 %
47: *n* = 10; 71 %

Scheme 10. Conjugation of pyrrole with cyclodextrin *via* an amide bond

High selectivity of CuAAC was used for the synthesis of the second group of Py-CD conjugates **48-50** connected *via* triazole ring (Scheme 11). The reaction between pyrrole **15** and 6^A-deoxy-6^A-azido-β-CD **35** was catalysed by 5 mol% of CuI and 2 eq. of DIPEA in DMF at 100 °C. Then, the crude reaction mixture was treated with TBAF, and the target molecule **48** was isolated in 61% yield after column chromatography on C-18 silica gel. Surprisingly the same reaction conditions applied for the compounds **20** and **21** did not lead to desired products. Therefore, a modified procedure published by Chmursky et al. was used instead.[43] The Cu(I) catalyst was generated *in situ* by reducing $CuSO_4$ with ascorbic acid while the system was further stabilised with 0.2 eq. of TBTA. The reaction proceeded in DMSO/H_2O mixture at 60 °C, thus under milder conditions. Triazoles **48-50** were purified by simple precipitation and isolated after the final deprotection step in 79-88% yields.

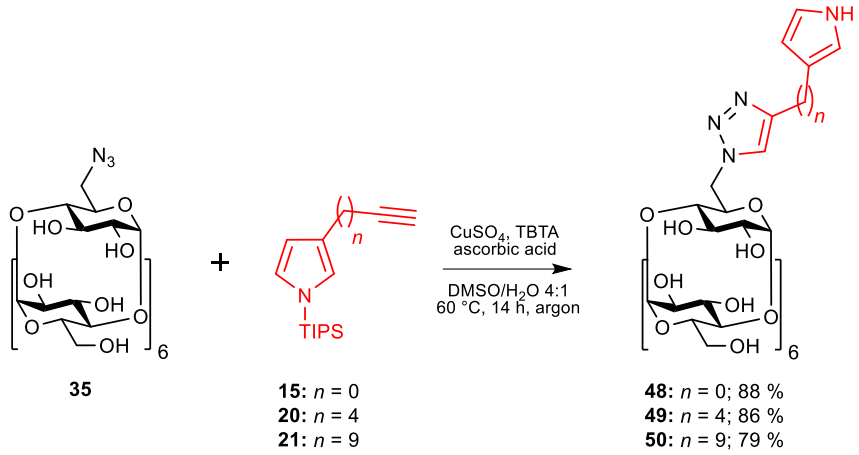

Scheme 11. Conjugation of pyrrole with cyclodextrin *via* triazole ring

3.4. Preparation of polypyrrole coating

3.4.1. Preparation of PPy film with carboxy or alkyne terminal groups

Previously synthesised Py-CD conjugates, **45-50** were used for initial polymerisations. The PCL fibrous substrate was prepared by electrospinning technique instead of drawing from the polymer droplet (Figure 4). Although oriented fibres are better for neural cell guidance, random fibrous material with μm fibres diameter (1.13 ± 0.36 μm) was used in this study for several objective reasons. One of them is that several square meters of PCL sheet could be easily prepared using the Nanospider® device compared to the tedious drawing technique. Moreover, samples are more robust, and the polymerisation is easily repeatable. Our first idea was to copolymerize CD-decorated pyrrole **45-50** together with pyrrole **1** under optimised reaction condition mentioned in the previous chapter. However, the polymerisation rate was much higher for the pyrrole **1,** and thus the pristine polypyrrole was created as an only product. The monomers **45-50** were polymerised separately as well but only starting material was detected using LC-MS even with prolonged reaction time or elevated temperature.

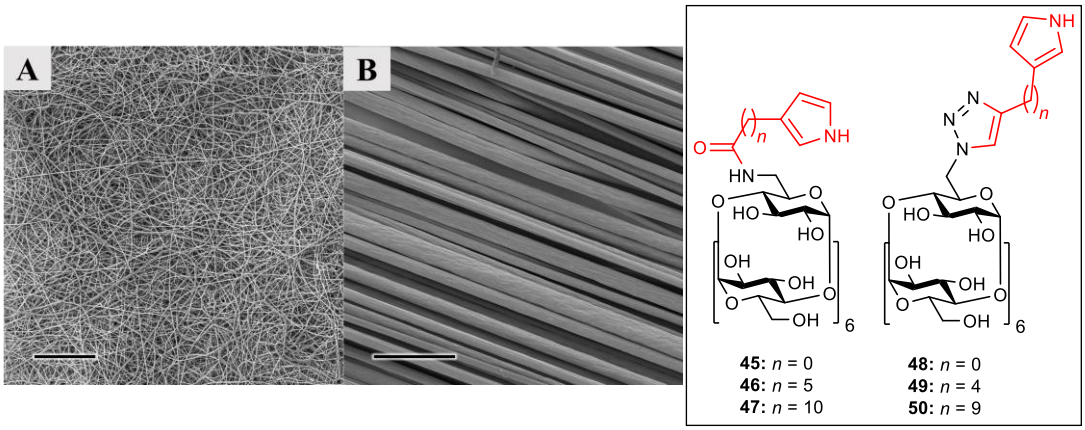

Figure 4. A, B) SEM image of PCL microfiber prepared by needless electrospinning and drawing technique (scale bar 100 μm); structures of β-substituted pyrrole monomers **45-50**

It is generally agreed, that substituted pyrroles polymerise slowly than unsubstituted analogues. It could be caused by steric demands of CD-Py monomer or interaction of the CD cavity with another molecule to form a stable supramolecular structure. For these reasons, we decided for the multistep procedure, where β-substituted pyrrole **28** or **30** with medium long carbon chain and various terminal group are deposited onto PCL surface, and then the cyclodextrin is connected using suitable conjugation reaction. Derivatives **28** or **30** were oxidised by $FeCl_3$ together with pyrrole **1** (ratio 1:1) in aqueous methanol to form a grey-black coating on the PCL matrix. Unexpected reactivity of β-substituted pyrroles **28** and **30** have been found which formed a copolymer with **1** in ratio 10:1 according to elemental analysis. We concluded, that

reaction rate is surprisingly high for pyrroles **28** or **30** and focused our efforts on the production of purely β-substituted conjugated polymers (Scheme 12) instead of polypyrrole copolymers. This approach led to the densely coated fibrous surface with a high amount of functional groups suitable for further derivatisation.

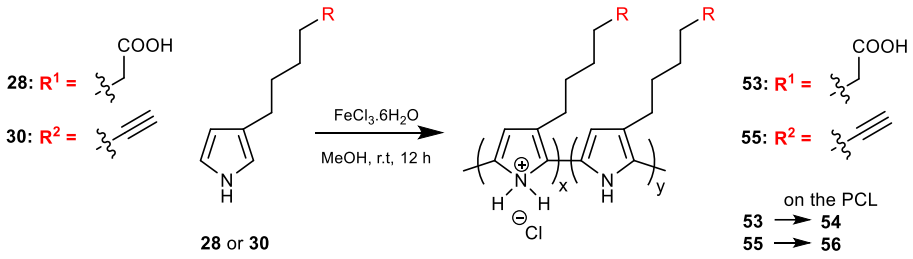

Scheme 12. Oxidation of pyrrole monomers **28** or **30** by $FeCl_3$ (PCL substrate omitted)

As could be seen in the SEM pictures below, the resulting PPy layer **53** formed on the PCL microfibers using 60% MeOH had many structural defect and agglomerates on the surface. Even 5 % of water content had a significant impact on surface morphology. Better wettability of PCL in methanol rendered smoothly coated material which precisely follows the surface structure. The unexpected high reactivity of substituted pyrrole **28** in MeOH was found which was in contrast to the observed behaviour of CD-substituted pyrroles **45-50**, published examples from the literature or even the reactivity of simple pyrrole **1**.

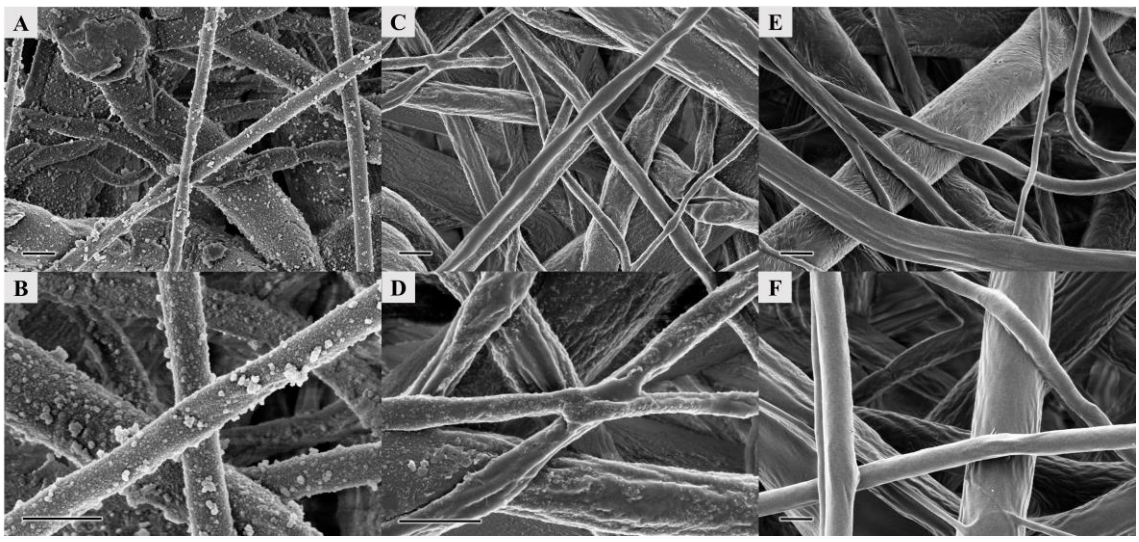

.

Figure 5. SEM image of the material **54**; **A, B)** 60% MeOH/H_2O (*v/v*); **C, D)** 95% MeOH/H_2O (*v/v*); **C, D)** 100% MeOH; scale bar 1 μm

The pristine polypyrrole **51** (blue line) has a limited number of characteristic vibrations in the IR if compared to its substituted analogues **53** and **55** (Figure 6). The first weak signal around 1700 cm^{-1} is probably vibration of conjugated π-system of the polymer backbone. It could be caused by the resonance of aromatic electrons to form imine like structures. The next signal at 1540 cm^{-1} is strong stretching vibrations of pyrrole ring followed by complicated deforming and skeletal vibrations at lower cm^{-1}. The red line in Figure 6 represents the IR spectrum of PPy-5C-COOH **53**. A broad valence vibration of carboxylic O-H group between 3500 – 3050 cm^{-1} and characteristic strong symmetrical stretching vibration of the C=O group confirm the presence of carboxylic acid in the polymer structure. Moreover, we can find symmetric as well as asymmetric vibrations of corresponding alkyl CH_2 linker at 2932 cm^{-1} and 2859 cm^{-1}.

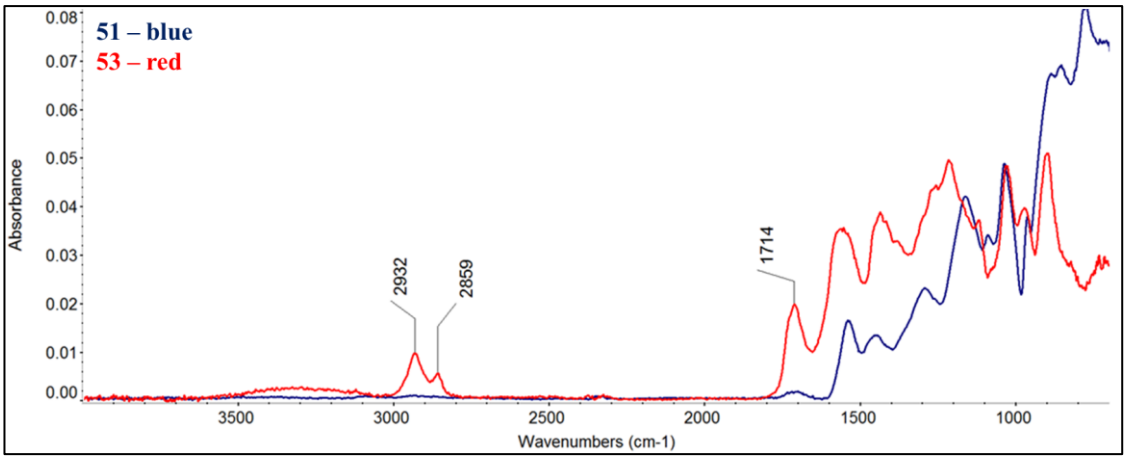

Figure 6. IR spectra of pristine PPy **51** and PPy **53** with carboxy groups

In the table below we can see that the resulting ratio of carbon to nitrogen corresponds accurately with the calculated values. Moreover, we were able to detect nitrogen in the both coated scaffolds **54** or **56** which confirmed the successful introduction of polypyrrole film on the surface of individual fibres.

Elemental analysis	**at% C** calcd / found	**at% H** calcd / found	**at% N** calcd / found	**C/N ratio** calcd / found
PPy 53	67.02 / 58.76	7.31 / 10.92	7.82 / 6.79	8.57 / 8.65
PPy 55	82.72 / 74.38	7.64 / 11.26	9.65 / 8.78	8.57 / 8.47

Table 1. Calculated and measured values of elemental composition for PPy **53** and **55**

Although the methods mentioned above provide valuable information about polymer composition, surface morphology and thermal properties, we still did not prove or estimated the amount of incorporated dopant. According to the published literature, this amount could vary significantly depending on the structure of doping agent, a method of polymer preparation. Small inorganic charged ions are incorporated more efficiently than large molecules, but the dopant exchange with moisture often occurs. We have prepared PCL-PPy composite materials using $FeCl_3$ as an oxidising agent in methanol to furnish coatings doped with chloride anion **53** or **55** based on EDS analysis (Figure 7). It is also generally agreed that some of the doped conductive polymers could find an application in tissue engineering. The interaction of CP with biological samples was described in several publications where the cytotoxicity was evaluated by extensive *in-vitro* and *in-vivo* experiments.[44-46]

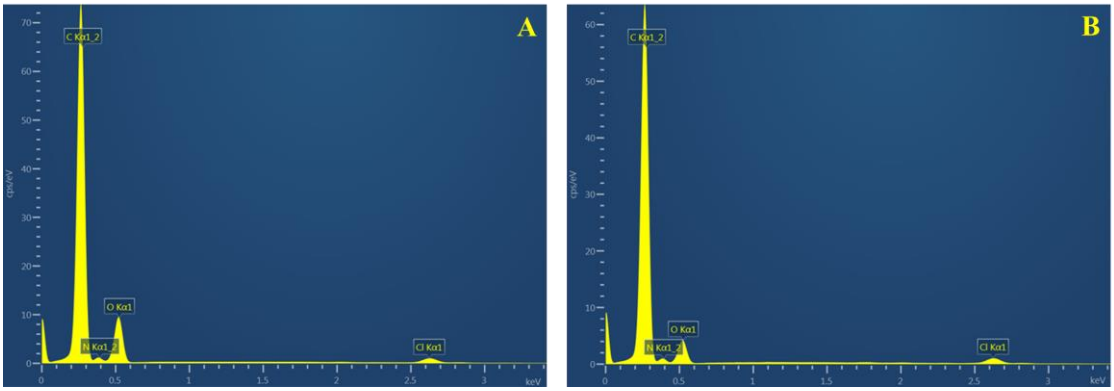

Figure 7. EDS spectra of polymers **A)** PPy **53** and **B)** PPy **55**

The chemical composition was affected by impurities caused by fast air moisture absorption, and thus oxygen could be found in both spectra. Although the overall values were shifted due to some impurities, the N/Cl ratio was independent on the material contamination and provided valuable information on the amount of dopant in the polymer structure (Table 2).

EDS	at% C	at% N	at% O	at% Cl	N/Cl molar ratio
PPy 53	79.02	5.40	14.85	0.73	7.40
PPy 55	83.84	6.66	8.62	0.89	7.48

Table 2. Elemental composition of PPy **53** and **55** measured by EDS

The level of doping was approximately one chlorine anion per every 7 – 8 pyrrole unit for the PPy **53**. The second sample **55** with aliphatic side chain had a similar level of doping. It means that we were able to prepare a series of polypyrrole composites with different side chains

suitable for various types of conjugation reactions but with the same level of doping. Hence, the *in-vitro* experiments should reflect more precisely the changes of the surface functionalization while the surface morphology and the level of doping are kept similar as possible.

The chemical composition of PPy layer **53** on the fibrous scaffold **54** was further studied by XPS method (Figure 8). Individual signals of the corresponding element were scanned separately with higher precision. As can be seen below, these signals are mostly a combination of the differently bound element. The blue line represents pristine PCL while the red lines are spectra of PCL-PPy-5C-COOH scaffold **54**. The oxygen and carbon spectra are similar for both samples because PCL substrate is measured together with thin PPy coating due to a higher penetration depth of incidental electrons. Even though, the oxygen and carbon spectra are not conclusive we can still rely on nitrogen spectrum because the nitrogen was not present in the pristine PCL. Although the polypyrrole typically has four binding modes in the nitrogen spectrum which correspond with the doped structure of the conductive polymer, we were able to distinguish only two modes. Nevertheless, despite the low intensity of measured spectrum the successful functionalization of PCL with PPy **53** has been confirmed. However, a more detailed study could shed light onto the binding modes of nitrogen and further describe a doping mechanism.

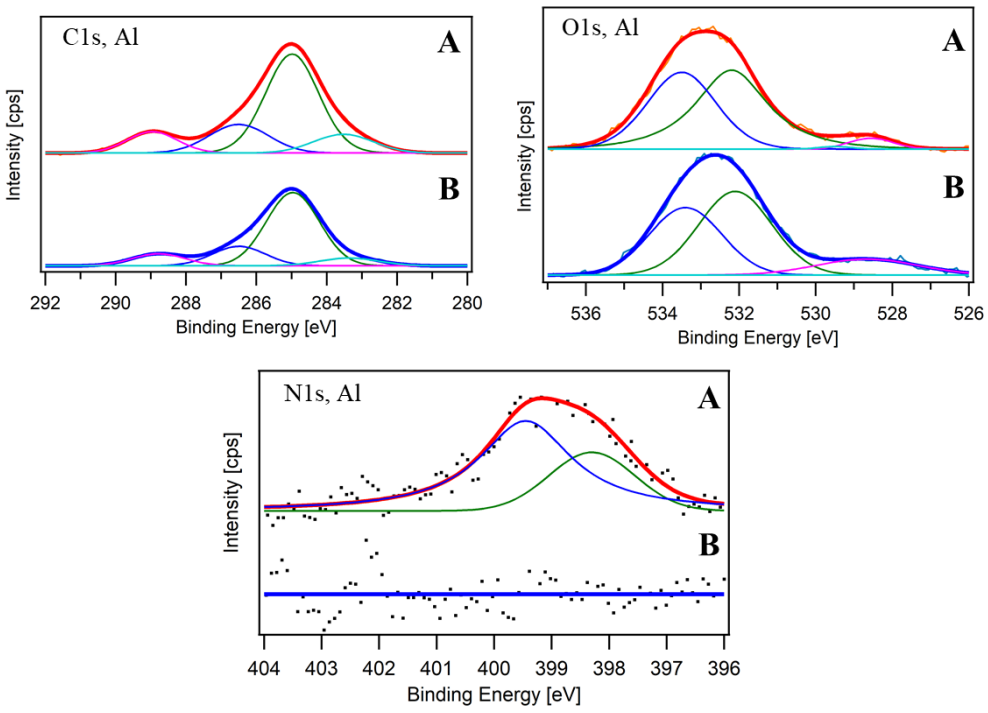

Figure 8. XPS spectra (C1s, O1s, N1s) of **A)** PPy **53**; **B)** pristine PCL

The chemical structure of PPy **53** in powder form was also studied by solid-state NMR (Figure 9). A similar molecule **57** was measured first as a standard (blue line) and compared with the sample of PPy **53** (red line). The solid-state ^{13}C NMR spectra were collected by rotating the sample under magic angle at 15 KHz. Both samples were measured at 303 K using a NMR machine operating at frequency 125.77 MHz. Then, expected chemical shifts were assigned to the corresponding carbon atoms. At 173.5 ppm the signal of COOH group could be found while the signals around 30 ppm are CH_2 carbons of the pyrrole aliphatic side chain. The carbons of the pyrrole ring are probably hidden under the signal between 155 – 95 ppm, where peak broadness is caused by a complicated conjugated system of double bonds in the polymer backbone. The chemical shift of the unassigned peak at 51.1 ppm suggests that this carbon is connected to the atom with higher electron density by a single bond. We could assume structure like -CH-NH- created on the α-carbons during doping but the chemical shift for carbocation should be significantly higher. The second explanation is based on the introduction of a particular structural defect, while the pyrrole ring is randomly connected with another heterocycle *via* the β-position.

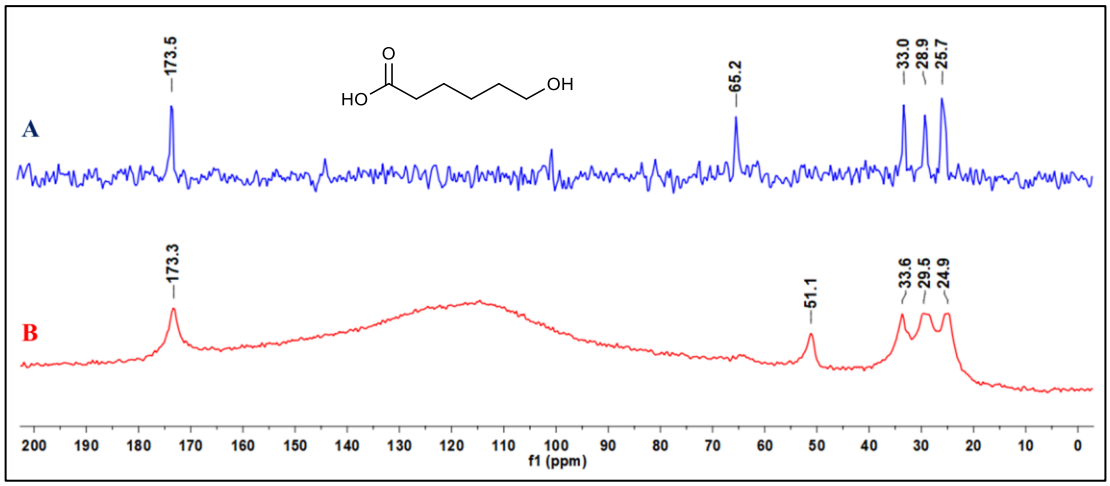

Figure 9. Solid-state ^{13}C MAS NMR spectra **A)** model compound; **B)** PPy **53**

For the summary, the structures of newly prepared polypyrrole derivatives were described and confirmed by several analytical techniques. Thermal properties of PPy **51**, **53**, **55** were studied, and the amount of deposited PPy on the PCL substrate was calculated based on TGA measurement for every sample. The polymerisation protocol for the deposition of PPy **53** or **55** was also optimised and the morphology of resulting scaffolds thoroughly examined using SEM.

3.4.2. Preparation of PCL-PPy scaffolds decorated with cyclodextrins

Our composite material **54** was decorated with cyclodextrins according to Scheme 13. The first step was the activation of carboxyl groups on the surface using EDC/NHS. It is generally agreed, that NHS forms a stable intermediate which is more resistant against hydrolysis but retains its reactivity and selectivity towards molecules containing amino groups. The reaction proceeded in MES buffer at pH 6 to keep high reactivity of activated ester and slow down the unwanted hydrolysis. After 3 hours of activation, the buffer was removed, and monosubstituted amino cyclodextrin **40**, **36** or **44** was added in 20 ml of fresh buffer. Finally, the activated substrate was shaken in aqueous buffer with the corresponding NH_2-CD at room temperature for 12 hours to yield functionalized materials. The washing procedure removed the excess of unreacted cyclodextrin together with some byproducts using an ultrasonic bath. All newly prepared materials PCL-5C-CONH- with immobilised α-CD **58**, β-CD **59** or γ-CD **60** on the surface were characterised and further used in biological experiments.

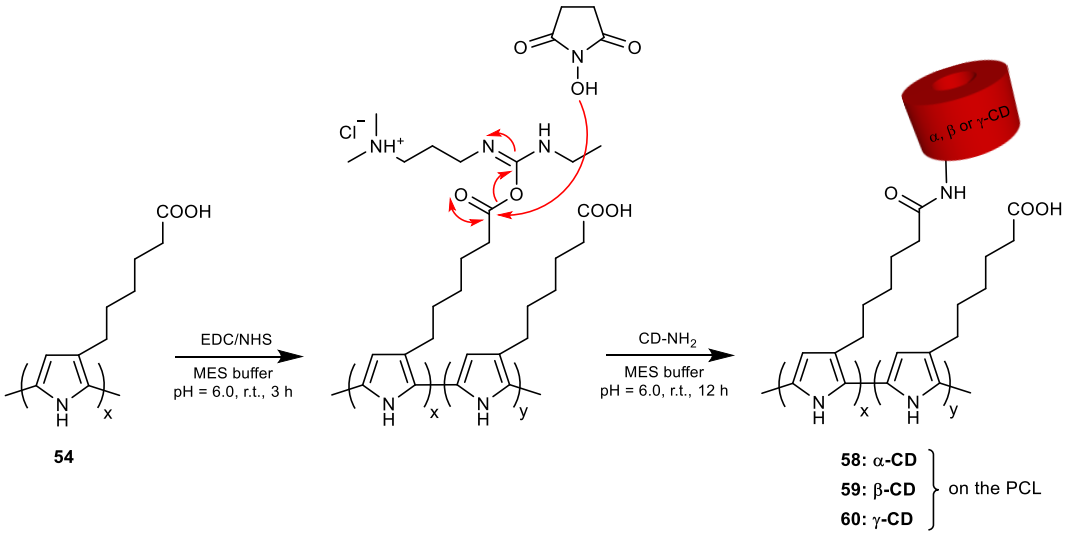

Scheme 13. Immobilisation of various CD using EDC/NHS (PCL substrate and doping agent omitted for better clarity)

Because of the low density of CD molecules on the surface, we had limited direct spectroscopic methods for its characterisation. However, it was estimated by fluorescence spectroscopy that the density of attached cyclodextrins on the PCL-PPy-5C-CONH-CD **59** was approximately 800 times lower than the maximal theoretical value. Although, this approach provided valuable information for the β-CD coated material **59** we were unable to determine the surface density of α- and γ-CD covered materials **58** and **60**. The reason was, that only β-CD interacts with Rhodamine B, while cavity of α-CD is too small for complexation and conversely inner space of γ-CD is broader than is necessary for strong host-guest interaction. At this point I

would allow an approximation, that surface density of bound α-, β- or γ-CD is about the same. If steric repulsion of CD is omitted due to low surface concentration and the reactivity of NH_2-CDs is roughly the same, the approximation as mentioned above is reasonable.

Further, the surface morphology of samples (PCL, PCL-PPy-5C-COOH **54**, PCL-PPy-5C-CONH-CD **58**, **59** and **60**) for *in-vitro* experiments were examined using SEM. We can see in Figure 10, that PCL matrix was coated with polypyrrole **53** without any significant surface defects. However, the longer polymerisation time (72 hours) had a slight impact on the mechanical properties of the final material, while a shorter reaction time (12 hours) afforded smoothly coated material without any surface defects or damaged fibres. The subsequent surface functionalization with cyclodextrins had no visible effect on the scaffold quality.

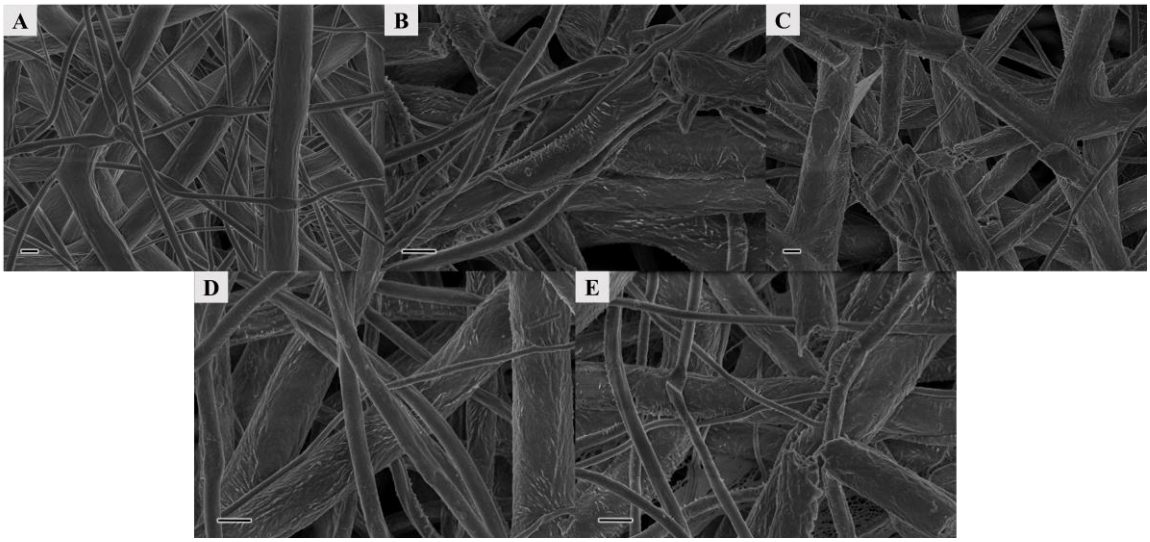

Figure 10. SEM image of **A)** PCL; **B)** PCL-PPy-5C-COOH **54**; **C)** PCL-PPy-5C-CONH-α-CD **58**; **D)** PCL-PPy-5C-CONH-β-CD **59**; **E)** PCL-PPy-5C-CONH-γ-CD **60**; scale bar 1 μm

Strongly hydrophobic neither hydrophilic materials are not favourable for cell adhesion and growth. Thus, we measured the water contact angle as an important parameter for all new materials. However, it can be found in the literature, that WCA is ranging by tens of degrees even for pristine fibrous PCL. It was difficult to distinguish whether the material morphology or surface chemistry has a stronger effect on WCA. Although we would like to compare WCA of tested materials, a small difference cannot be distinguished for the nonwoven scaffolds. The interpretation of such results is difficult due to variable fibres density which significantly affects the value of measured contact angle. Thus, we have focused our attention on the parameters, which could be measured more precisely for the given materials.

3.4.2.1. Biological experiments on functionalized PCL scaffolds

The main goal of this thesis is design, preparation, characterisation and biological evaluation of new molecular scaffold for tissue engineering. While properties of PCL-PPy fibrous materials were thoroughly described in the previous chapter, this part will be focused on cell-material interaction. At this point, we will focus on the *in-vitro* experiments to study the biocompatibility of newly prepared materials. Later it will be necessary to investigate the degradation profiles, byproducts formation or potentially toxic compounds leaching as well.

Five fibrous materials **A-E** were subjected to an *in-vitro* experiment with NHDF cell line, and the cell metabolic activity was determined using the MTT assay over two weeks (Graph 1). This assay is based on the transformation of yellow tetrazolium dye by mitochondrial reductase enzyme into purple formazan. Then, the absorbance is measured at a specific wavelength, and the number of viable cells is quantified according to the calibration curve. The data clearly show, that PPy coating **53** is not only biologically compatible but also significantly improves cell growth. Moreover, the introduction of cyclodextrins further increases overall performance. On the other hand, only a minor change in cell viability can be seen between materials bearing different types of cyclodextrins on the surface.

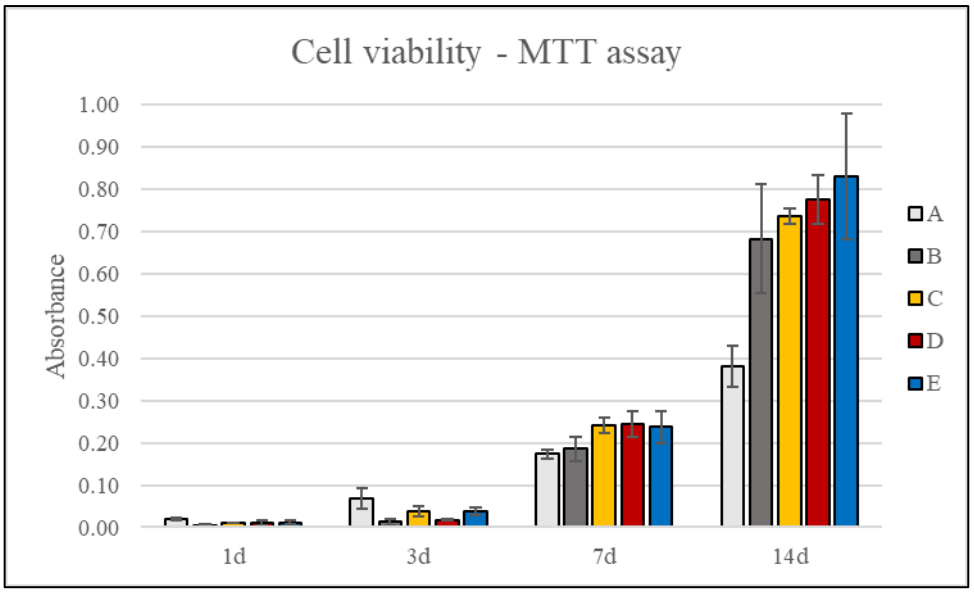

Graph 1. Cell metabolic activity (MTT assay) **A)** PCL; **B)** PCL-PPy-5C-COOH **54**; **C)** PCL-PPy-5C-CONH-α-CD **58**; **D)** PCL-PPy-5C-CONH-β-CD **59**; **E)** PCL-PPy-5C-CONH-γ-CD **60**

Thanks to these results our original goal of creating material combining cues for cell adhesion, proliferation and growth has been pushed forward. The introduction of cyclodextrin macrocycles onto a polymer surface probably worked thanks to host-guest interaction between

the CD cavity and ECM synergistically. Although these non-bonding interactions are relatively weak, they have a dramatic impact on protein adhesion and subsequent cell viability. For the first few days, a higher cellular activity has been seen on the pristine PCL if compared to other tested samples. Cells were well spread on the fibres which had a direct effect on their growth based on the SEM images. Although cell activity was better on pristine PCL during the first days of the *in-vitro* experiment, later there was a sharp increase in the number of cells on the functionalized substrates. The first reason could be the interaction of ECM with charged PPy surface and thus better cell-cell communication *via* conductive polymer backbone. Secondly, inclusion complexes of serum proteins with lipophilic CD cavity could provide binding sites for cell adhesion and boost the cell-material interaction. Hence, the importance of surface chemistry was demonstrated on protein absorption experimentally. Generally known fact, that material surface is covered with adhesive protein before cell attachment leads us to such specifically designed scaffold at the first place. While many different proteins were already present in the culturing media, we just exploited CD ability to form inclusion complexes and to pull up proteins onto the surface. This action was followed by dynamic surface layer remodelling and later to cell adhesion *via* specific receptors. Although surface coating with RGD amino acid sequence[104] represents the most common strategy, our approach relies on spontaneous interaction of the CD cavity with proteins to form a tissue mimicking environment.

The promising results from the *in-vitro* experiment showed that surface functionalization has a dramatic impact on cell proliferation, maturation and growth. Although there are many factors which simultaneously influence the overall cell response we focused our attention on the protein adhesion. It is known, that adhesion-mediating proteins like fibronectin, vitronectin or laminin adsorb onto the material surface, and the specific cell membrane receptors then recognise their presence. After this initial phase, the attached cells begin to feel the surface chemistry, topography and roughness and adapt their life cycle according to the given stimulus.

Interestingly, even the low concentration of CD on the surface dramatically improves cell proliferation, spreading, differentiation and growth. This phenomenon could be caused by the favourable interaction with the adhesion-mediating proteins which are absorbed on the surface in non-denatured conformation. Such naturally organised surface is more favourable for cell attachment which ultimately improves scaffold performance.

3.4.3. Preparation of PCL-PPy composites with the tuneable linker

In the next stage of our research, the influence of carbon linker length on cell growth was examined. Before the biological experiment, the polymerisation of pyrrole **27**-**29** was studied (Scheme 14). While the oxidation of pyrrole **28** and **29** proceeded smoothly, the pyrrole derivative **27** with carboxyl group connected directly to the heterocycle did not react under similar conditions. However, if the water was used as a solvent, the monomer **27** was finally deposited onto PCL at 45 °C. At this temperature the reaction was tedious, and it took 3 days before some visual change was visible. Moreover, the reaction worked swiftly at 95 °C, but the PCL substrate would be melted at this temperature.

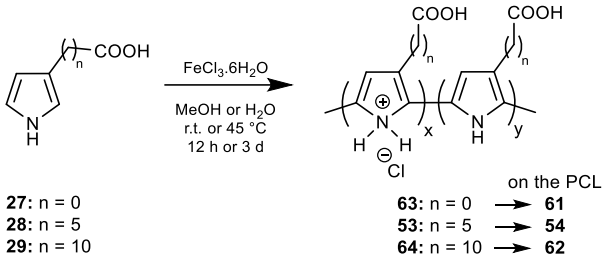

Scheme 14. Oxidation of pyrrole monomers **27**-**29** by $FeCl_3$ (PCL substrate omitted)

The morphology of PCL-PPy scaffolds **61** (Figure 11), **54**, **62** (Figure 13) was examined using SEM and the deposited PPy layers **53**, **63** and **64** were characterised by elemental analysis, IR or TGA in powdered form. A surprising structure of PCL-PPy-OC-COOH **61** can be seen in the picture below. While pristine PCL fibrous scaffold represents material with a regular surface, the morphology of resulting composite **61** after PPy **63** deposition has changed considerably. This example clearly illustrates how the type of solvent, the reaction temperature or minor change in monomer structure could influence the quality of final material. Probably a different wettability of PCL in water/methanol or the polymerisation rate were responsible for this unexpected outcome. Moreover, a significant amount of hematite side product was incorporated in the material structure despite an extensive washing procedure. Regularly, PPy coated substrates have grey-black colour, but sample **61** was reddish-brown (hematite). Moreover, EDS analysis confirmed a presence of residual Fe in the spectrum which also corresponded with the TGA analysis.

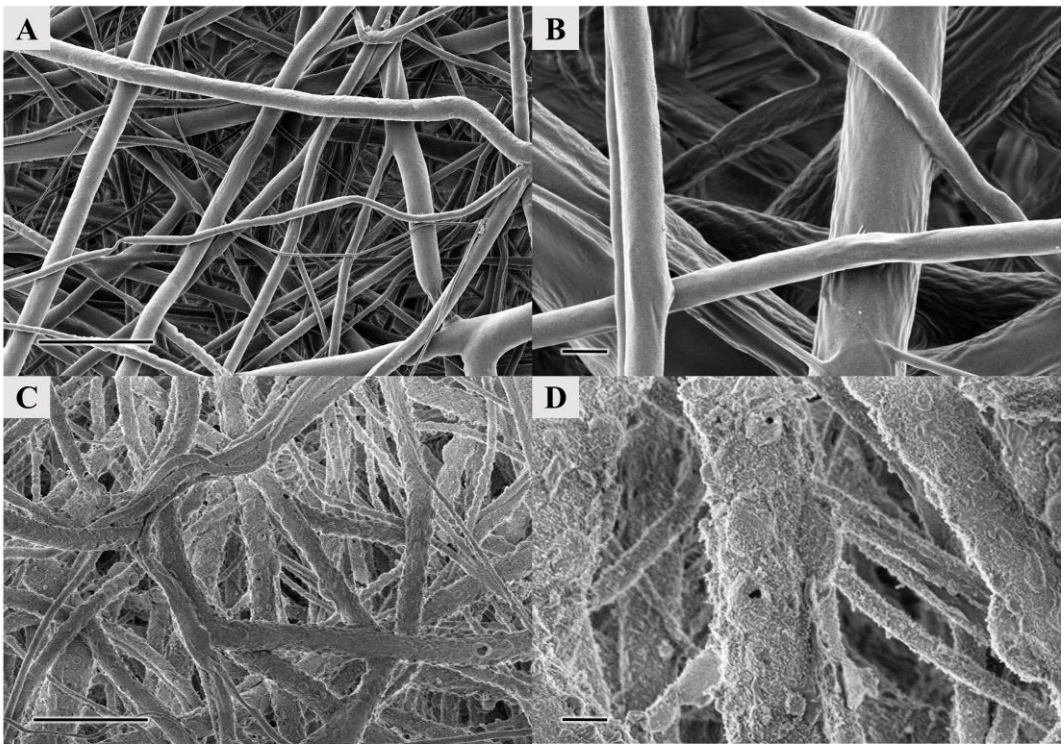

Figure 11. SEM images of **A, B)** pristine PCL; **C, D)** PCL-PPy-OC-COOH **61**; scale bar 1 μm

Thermal properties were investigated only for polypyrroles **53** and **64** with carbon linkers (Figure 12). Our goal was to prove the presence of PPy on the surface and also calculate the amount of deposited PPy. Although, the majority of weight loss was the contribution of PCL we could still calculate the amount of deposited polypyrrole from residual weights. Thus, pristine PCL, PCL-PPy scaffold (**54** or **62**) and powdered PPy (**53** or **64**) were measured separately. The difference in residual weights of pristine PCL and functionalized materials were 1.98 % (PCL-PPy-5C-COOH **54**) and 2.46 % (PCL-PPy-10C-COOH **62**). If some approximations were taken into account, the PCL-PPy scaffolds **54** and **62** contained 5.0 wt% of PPy **53** and 7.9 wt% of PPy **64** on the surface (see experimental part). This conclusion correlated with observed reactivity of monomer **29** which provided darker PCL fibrous material **62** if compared to other samples. Although such a method could not tell us about the thickness of PPy layer without known density, we have established fast and reliable proof of PPy deposition. Moreover, the amount of surface-bound PPy from different experiments can be easily compared.

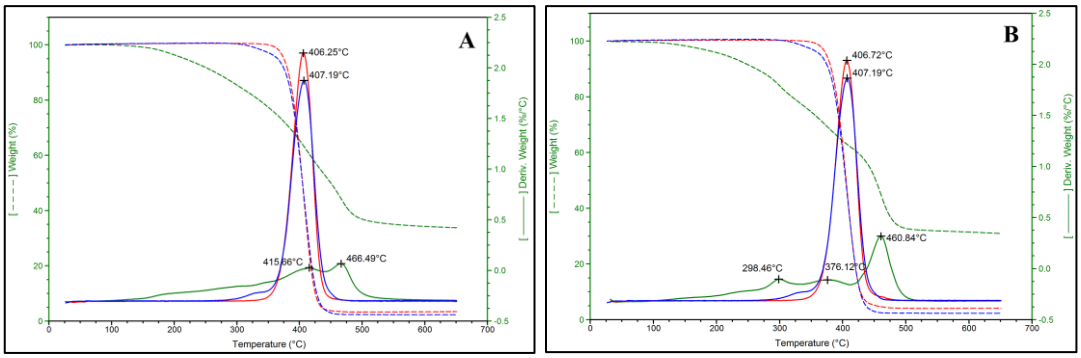

Figure 12. TGA spectra of **A)** PCL (blue), PCL-PPy **54** (red), PPy **53** (green); **B)** PCL (blue), PCL-PPy **62** (red), PPy **64** (green)

Further, composite scaffolds **54** and **62** were functionalized with β-CD **36** while the reaction conditions for CD immobilisation were taken over the previous experiment (Scheme 15). First, all available surface bound carboxyl groups were activated using EDC/NHS, then the β-CD **36** was added to furnish the desired materials. Although the main product should be an amide, the competing reaction is always hydrolysis, especially in more acidic water solution. Even though some activated carboxyl groups were hydrolysed the successful introduction of CDs onto PPy surface was confirmed by fluorescence spectroscopy using host-guest labelling technique as mentioned previously. The surface density of immobilised CDs was similar for both samples which allowed us to study cell viability on the CD decorated materials connected to the surface *via* differently long carbon linkers.

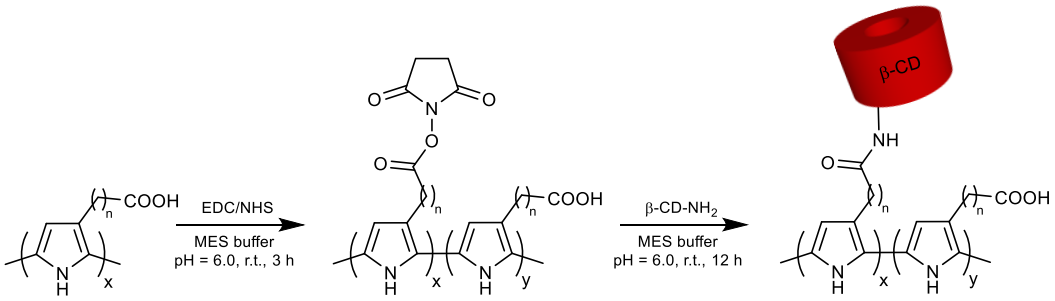

Scheme 15. Immobilisation of β-CD using EDC/NHS in MES buffer (PCL substrate and the doping agent were omitted for better clarity)

The structure and surface morphology of samples **59** and **65** were studied using scanning electron microscopy and compared with PCL-PPy **54**, **62** before functionalization. All individual fibres were smoothly coated without any defects as can be seen in the images below (Figure 13). For a summary, the protocol for CD connection utilising the classical carbodiimide chemistry can be also applied for the connection of CD onto PPy **62**. Although a longer carbon linker could interact with CD lipophilic cavity and thus hinder conjugation *via* an amide bond, the surface density of immobilized β-CD was similar for both samples **54** or **62**.

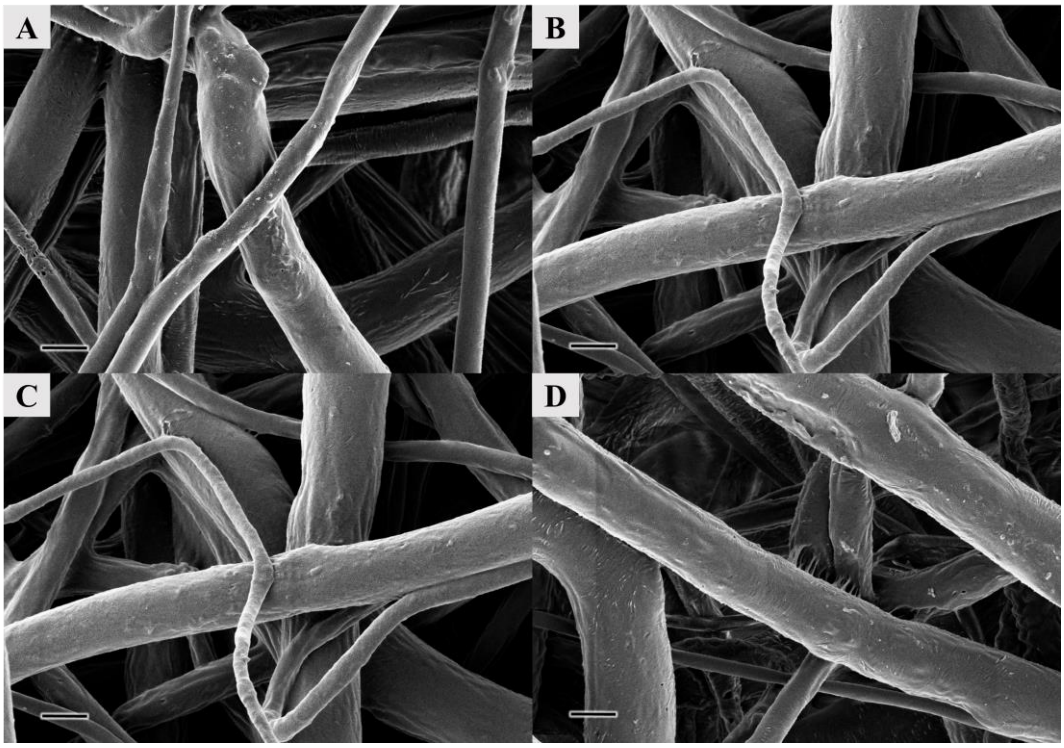

Figure 13. SEM images of **A)** PCL-PPy-5C-COOH **54**; **B)** PCL-PPy-5C-CONH-β-CD **59**; **C)** PCL-PPy-10C-COOH **62**; **D)** PCL-PPy-10C-CONH-β-CD **65**; scale bar 1 μm

There is a question if flexible carbon linker increases CD ability to form inclusion complexes with serum protein and thus improves cell adhesion, or its more lipophilic character hampers desirable molecular recognition. Therefore, the *in-vitro* experiment was carried out to further understand the behaviour of our new material in contact with biological matter. The experiment was carried out for 14 days with NHDF cells complementary to the previous *in-vitro* experiment. The results of cell viability are summarized in Graph 2 below where the same pattern as before (Graph 1) could be seen. Although the cell metabolic activity of NHDF on the pristine PCL seemed better during the first days of the *in-vitro* experiment, it was greatly surpassed by functionalized materials later.

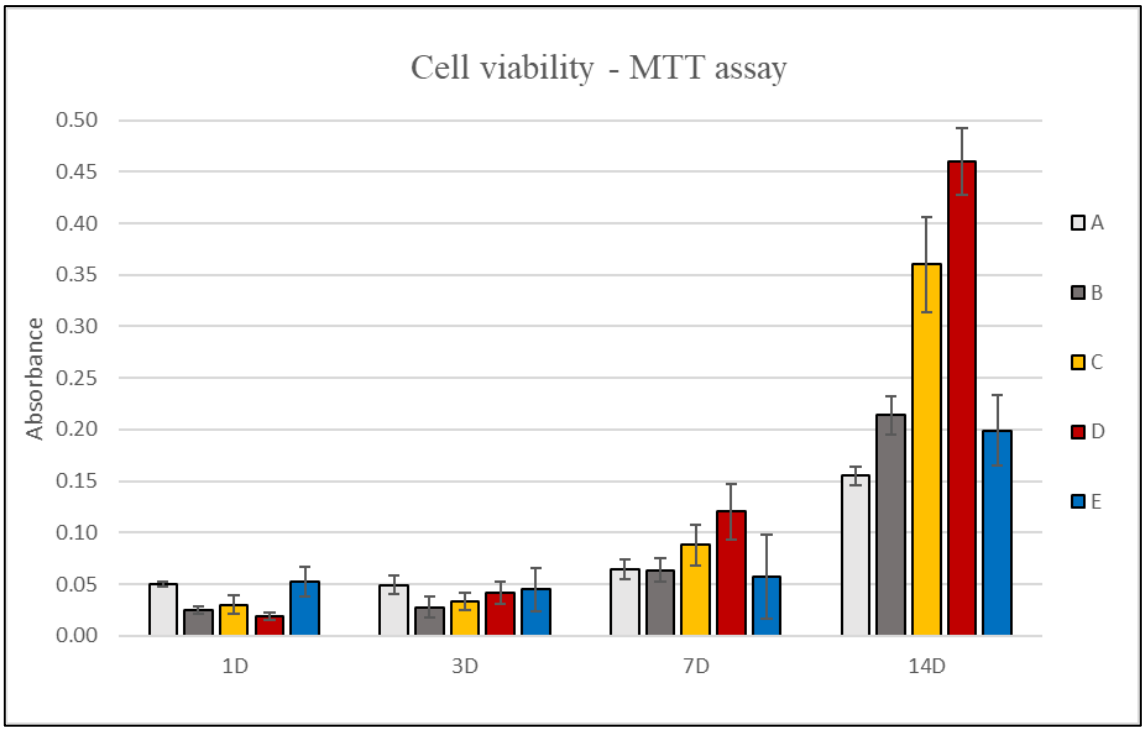

Graph 2. Cell metabolic activity (MTT assay) **A)** PCL; **B)** PCL-PPy-5C-COOH **54**; **C)** PCL-PPy-10C-COOH **62**; **D)** PCL-PPy-5C-CONH-β-CD **59**; **E)** PCL-PPy-10C-CONH-β-CD **65**

If the results are analysed, several conclusions about cell interaction with the fibrous scaffolds can be formulated. Generally, all functionalized materials have a positive effect on the cell adhesion, proliferation and growth. Based on SEM images, cells were well spread and also incorporated in the fibrous structure. Similar data have been obtained from two separate *in-vitro* experiments for PCL, PCL-5C-COOH **54** and PCL-PPy-5C-CONH-β-CD **59** scaffolds. Further, an unexpected behaviour was found for the β-CD functionalized material **65** where its performance was only 28 % better than pristine PCL but surprisingly 81% worse than PCL-PPy composite **62** without β-CD on the surface. On the other hand, in the case of sample **59**, there was almost 200 % increase in cell metabolic activity compared to PCL. Although the cell growth was also better (38 %) on the PCL-PPy **54** compared to PCL the decisive positive influence of β-CD on the cell adhesion and growth has been proved. This result is also fascinating because the attached cyclodextrins have a significant effect on cell activity even in at low surface concentration.

4. CONCLUSION

The targets of this work have been achieved by systematic work on the well-scheduled project, excellent mentoring and collaboration with many capable colleagues. In the beginning, we focused our attention on the synthesis of β-substituted pyrrole derivatives suitable for the cyclodextrin attachment. The most challenging task was to overcome an instability of some β-substituted pyrroles and find multistep reaction sequences leading to the essential intermediates. New pyrroles with iodo, cyano, azido, carbonyl, a carboxyl group or multiple terminal bond have been synthesised and spectroscopically characterised during ongoing research. Although the conjugation procedures using selective amide bond or triazole formation for cyclodextrin connection were found, the subsequent polymerisation of such bulky monomers did not proceed as expected. Therefore, suitable pyrrole monomers with a carboxy group or triple bond on carbon linker have been synthesised and later polymerised onto the fibrous PCL matrix. At first, the ideal ratio of pyrrole/oxidant/dopant in the polymerisation solution, reaction time, temperature and washing protocol were optimised on the drawn PCL fibres. Then, the procedure has been slightly changed for the deposition of functionalized PPy derivatives onto the random electrospun fibrous matrix. SEM confirmed the morphology of newly prepared materials, and the chemical structure of PPy coating was determinate using elemental analysis, IR spectroscopy, solid-state NMR, EDS or XPS. Moreover, the amount of deposited polypyrrole was quantified by TGA which has proven to be a fast and reliable method for the confirmation of successful polypyrrole deposition.

A crucial part of this thesis was the following introduction of cyclodextrins onto the core-shell PCL-PPy fibrous samples. The surface was decorated with cyclodextrins *via* the amide bond, and the number of immobilised molecules was indirectly measured by fluorescence spectroscopy. Finally, *in-vitro* experiments were used to compare the influence of surface-bound α-, β- or γ-CD on cell growth. Results suggest that PCL-PPy-CD material supports cell proliferation and growth much more than pristine PCL. However, there was no significant difference between α-, β- or γ-CD functionalized scaffolds. The effect of carbon spacer length separating the cyclodextrin from the surface on the NHDF cells growth was also compared. It can be said that less flexible linkers are preferable which is in good agreement with published literature. The original idea behind this work was to create a scaffold which supports proteins absorption and thus improves the overall cell-material interaction. An interesting finding concerning the results of *in-vitro* experiments is, that pristine PCL is superior for the protein absorption compared to functionalized samples. Nevertheless, the spatial conformation of adsorbed proteins is a far more critical parameter for the cell adhesion. Therefore, a complex study and a deeper understanding of this phenomenon would be interesting in the future.

To expand the possibilities of material functionalization, four other electrospun fibrous polymers (PDX, P4HB, PA6 and PVDF) were coated by PPy derivative under similar conditions

as described above. The amount of deposited PPy was experimentally determined and the morphology of resulting materials analysed by SEM. Besides, newly synthesised pyrrole monomers with double or triple bond were polymerised as well which further extended the possibility of surface functionalization. Huisgen dipolar cycloaddition is widely used in the field of material derivatisation even though thiol-ene/yne reactions represent a straightforward and highly selective method to utilise. This type of photo-induced reaction would bring another advantage for biomolecules immobilisation in the future. Moreover, the combination of a 3D polymeric matrix with a deposited conductive polypyrrole layer offers the opportunity to study the effect of conductivity on cell growth. Although this plan looks simple, it will be essential to find suitable polypyrrole/dopant combination with desirable conductivity, biocompatibility and superior environmental stability.

5. ABBREVIATIONS AND SYMBOLS

BSA	Bovine serum albumin
CD	Cyclodextrin
COSY	Correlation spectroscopy
CuAAC	Copper catalysed azide-alkyne cycloaddtion
DBSA	Dodecylbenzensulfonic acid
DIBAH	Diisobutylaluminium hydride
DIPEA	*N*,*N*-Diisopropylethylamine
DMSO	Dimethylsulfoxide
ECM	Extracellular matrix
EDC	*N*-(3-Dimethylaminopropyl)-*N*-ethylcarbodiimide hydrochloride
eq.	Equivalent
GC-MS	Gas chromatography with mass detection
GPC	Gel permeation chromatography
HMBC	Heteronuclear multiple-bond correlation spectroscopy
HRMS	High resolution mass spectroscopy
HSQC	Heteronuclear single-quantum correlation spectroscopy
LDA	Lithium diisopropylamide
LC-MS	Liquid chromatography with mass detection
MeOH	Methanol
MES	2-(*N*-morpholino)ethanesulfonic acid
MO	Methyl orange
NBS	*N*-Bromosuccinimide
n-BuLi	*n*-Butyl lithium
NHDF	Normal dermal human fibroblast
NHS	*N*-hydroxysuccinimide
NIS	*N*-Iodosuccinimide
NMR	Nuclear magnetic resonance
PA6	Polyamide 6 (Nylon)
PCL	Polycaprolactone
PDX	Polydioxanone

P4HB	Polyhydroxybutyrate
PLA	Polylactic acid
ppm	Parts per million
PPy	Polypyrrole
PS	Polystyrerne
PVDF	Polyvinylidenedifluoride
PyBOP	(Benzotriazol-1-yloxy)tripyrrolidinophosphonium hexafluorophosphate
Rh B	Rhodamine B
rpm	Rotations per minute
RT	Room temperature
SDS-PAGE	Sodium dodecyl sulphate – polyacrylamide gel electrophoresis
S_EAr	Electrophilic aromatic substitution
SEM	Scanning electron microscopy
S_N2	Nucleophilic substitution bimolecular
TBAF	Tetrabutylamonium fluoride
TBTA	Tris[(1-benzyl-1H-1,2,3-triazol-4-yl)methyl]amine
t-BuLi	*terc*-Butyl lithium
TGA	Thermogravimetric analysis
THAT	Tris(3-hydroxypropyltriazolylmethyl)amine
THF	Tetrahydrofuran
TIPS	Triisopropylsilyl
TMS	Trimethylsilyl
Ts	*para*-Toluensulfonyl
UV/VIS	Spectroscopy in ultra violet or visible part of the spectrum
WCA	Water contact angle

6. LITERATURE

(1) Hantzsch, A. Neue Bildungsweise von Pyrrolderivaten. *Berichte Dtsch. Chem. Ges.* **1890**, *23* (1), 1474–1476.

(2) Knorr, L. Synthese von Pyrrolderivaten. *Berichte Dtsch. Chem. Ges.* **1884**, *17* (2), 1635–1642.

(3) Paal, C. Ueber Die Derivate Des Acetophenonacetessigesters Und Des Acetonylacetessigesters. *Berichte Dtsch. Chem. Ges.* **1884**, *17* (2), 2756–2767.

(4) Estevez, V.; Villacampa, M.; Menendez, J. C. Recent Advances in the Synthesis of Pyrroles by Multicomponent Reactions. *Chem. Soc. Rev.* **2014**, *43* (13), 4633–4657.

(5) Bhardwaj, V.; Gumber, D.; Abbot, V.; Dhiman, S.; Sharma, P. Pyrrole: A Resourceful Small Molecule in Key Medicinal Hetero-Aromatics. *Rsc Adv.* **2015**, *5* (20), 15233–15266.

(6) O'Hagan, D. Pyrrole, Pyrrolidine, Pyridine, Piperidine and Tropane Alkaloids. *Nat. Prod. Rep.* **2000**, *17* (5), 435–446.

(7) De Rosa, M. Chlorination of Pyrrole. N-Chloropyrrole: Formation and Rearrangement to 2- and 3-Chloropyrrole. *J. Org. Chem.* **1982**, *47* (6), 1008–1010.

(8) Alvarez, A.; Guzman, A.; Ruiz, A.; Velarde, E.; Muchowski, J. Synthesis of 3-Arylpyrroles and 3-Pyrrolylacetylenes by Palladium-Catalyzed Coupling Reactions. *J. Org. Chem.* **1992**, *57* (6), 1653–1656.

(9) Zonta, C.; Fabris, F.; De Lucchi, O. The Pyrrole Approach toward the Synthesis of Fully Functionalized Cup-Shaped Molecules. *Org. Lett.* **2005**, *7* (6), 1003–1006.

(10) Bray, B.; Mathies, P.; Naef, R.; Solas, D.; Tidwell, T.; Artis, D.; Muchowski, J. N-(Triisopropylsilyl)Pyrrole - a Progenitor Par Excellence of 3-Substituted Pyrroles. *J. Org. Chem.* **1990**, *55* (26), 6317–6328.

(11) Kakushima, M.; Hamel, P.; Frenette, R.; Rokach, J. Regioselective Synthesis of Acylpyrroles. *J. Org. Chem.* **1983**, *48* (19), 3214–3219.

(12) Anderson, H.; Loader, C.; Xu, R.; Le, N.; Gogan, N.; Mcdonald, R.; Edwards, L. Pyrrole Chemistry .28. Substitution-Reactions of 1-(Phenylsulfonyl)Pyrrole and Some Derivatives. *Can. J. Chem.-Rev. Can. Chim.* **1985**, *63* (4), 896–902.

(13) Jolicoeur, B.; Chapman, E. E.; Thompson, A.; Lubell, W. D. Pyrrole Protection. *Tetrahedron* **2006**, *62* (50), 11531–11563.

(14) Fukuda, T.; Ohta, T.; Sudo, E.; Iwao, M. Directed Lithiation of N-Benzenesulfonyl-3-Bromopyrrole. Electrophile-Controlled Regioselective Functionalization via Dynamic Equilibrium between C-2 and C-5 Lithio Species. *Org. Lett.* **2010**, *12* (12), 2734–2737.

(15) Pickup, P. G. Alternating Current Impedance Study of a Polypyrrole-Based Anion-Exchange Polymer. *J. Chem. Soc. Faraday Trans.* **1990**, *86* (21), 3631–3636.

(16) Greene, R. L.; Street, G. B.; Suter, L. J. Superconductivity in Polysulfur Nitride. *Phys. Rev. Lett.* **1975**, *34* (10), 577–579.

(17) Ito, T.; Shirakawa, H.; Ikeda, S. Simultaneous Polymerization and Formation of Polyacetylene Film on Surface of Concentrated Soluble Ziegler-Type Catalyst Solution. *J. Polym. Sci. Part -Polym. Chem.* **1974**, *12* (1), 11–20.

(18) Shirakawa, H.; Louis, E. J.; MacDiarmid, A. G.; Chiang, C. K.; Heeger, A. J. Synthesis of Electrically Conducting Organic Polymers: Halogen Derivatives of Polyacetylene, (CH)x. *J. Chem. Soc. Chem. Commun.* **1977**, *0* (16), 578–580.

(19) MacDiarmid, A. G. "Synthetic Metals": A Novel Role for Organic Polymers (Nobel Lecture). *Angew. Chem.-Int. Ed.* **2001**, *40* (14), 2581–2590.

(20) Snook, G. A.; Kao, P.; Best, A. S. Conducting-Polymer-Based Supercapacitor Devices and Electrodes. *J. Power Sources* **2011**, *196* (1), 1–12.

(21) Pron, A.; Rannou, P. Processible Conjugated Polymers: From Organic Semiconductors to Organic Metals and Superconductors. *Prog. Polym. Sci.* **2002**, *27* (1), 135–190.

(22) Kumar, D.; Sharma, R. C. Advances in Conductive Polymers. *Eur. Polym. J.* **1998**, *34* (8), 1053–1060.

(23) McQuade, D. T.; Pullen, A. E.; Swager, T. M. Conjugated Polymer-Based Chemical Sensors. *Chem. Rev.* **2000**, *100* (7), 2537–2574.

(24) Guimard, N. K.; Gomez, N.; Schmidt, C. E. Conducting Polymers in Biomedical Engineering. *Prog. Polym. Sci.* **2007**, *32* (8–9), 876–921.

(25) Ratner, B. D. The Biocompatibility Manifesto: Biocompatibility for the Twenty-First Century. *J Cardiovasc. Transl. Res.* **2011**, *4* (5), 523–527.

(26) Stefan, K.; Schuhmann, W.; Parlar, H.; Korte, F. Synthesis of New 3-Substituted Pyrroles. *Chem. Ber.* **1989**, *122* (1), 169–174.

(27) Kolb, H. C.; Finn, M. G.; Sharpless, K. B. Click Chemistry: Diverse Chemical Function from a Few Good Reactions. *Angew. Chem.-Int. Ed.* **2001**, *40* (11), 2004–2021.

(28) Kolb, H. C.; Sharpless, K. B. The Growing Impact of Click Chemistry on Drug Discovery. *Drug Discov. Today* **2003**, *8* (24), 1128–1137.

(29) Huisgen, R. 1.3-Dipolare Cycloadditionen - Ruckschau Und Ausblick. *Angew. Chem.-Int. Ed.* **1963**, *75* (13), 604–637.

(30) Biffis, A.; Centomo, P.; Del Zotto, A.; Zecca, M. Pd Metal Catalysts for Cross-Couplings and Related Reactions in the 21st Century: A Critical Review. *Chem. Rev.* **2018**, *118* (4), 2249–2295.

(31) Heravi, M. M.; Hajiabbasi, P. Recent Advances in Kumada-Tamao-Corriu Cross-Coupling Reaction Catalyzed by Different Ligands. *Monatshefte Chem.* **2012**, *143* (12), 1575–1592.

(32) Negishi, E.; Kotora, M.; Xu, C. D. Direct Synthesis of Terminal Alkynes via Pd-Catalyzed Cross Coupling of Aryl and Alkenyl Halides with Ethynylmetals Containing Zn, Mg, and Sn. Critical Comparison of Counteractions. *J. Org. Chem.* **1997**, *62* (25), 8957–8960.

(33) Yang, L. M.; Huang, L. F.; Luh, T. Y. Kumada-Corriu Reactions of Alkyl Halides with Alkynyl Nucleophiles. *Org. Lett.* **2004**, *6* (9), 1461–1463.

(34) Rutledge, T. Sodium Acetylide .2. Reactions of Sodium Acetylide in Organic Diluents - Preparation of Monoalkyl Acetylenes. *J. Org. Chem.* **1959**, *24* (6), 840–842.

(35) Smith, W.; Beumel, O. Preparation of Alkynes and Dialkynes by Reaction of Monohalo-Alkanes and Dihaloalkanes with Lithium Acetylenide-Ethylenediamine Complex. *Synth.-Stuttg.* **1974**, No. 6, 441–442.

(36) Corey, E.; Fuchs, P. Synthetic Method for Formyl Ethynyl Conversion (Rcho-Rc=ch or Rc=cr'). *Tetrahedron Lett.* **1972**, No. 36, 3769-3772.

(37) Brown, H.; Garg, C. Selective Reductions. .4. Partial Reduction of Nitriles with Lithium Triethoxyaluminohydride-Convenient Aldehyde Synthesis. *J. Am. Chem. Soc.* **1964**, *86* (6), 1085-1089.

(38) Miller, A.; Biss, J.; Schwartzman, L. Reductions with Dialkylaluminum Hydrides. *J. Org. Chem.* **1959**, *24* (5), 627–630.

(39) Kornblum, N.; Jones, W.; Anderson, G. A New and Selective Method of Oxidation - the Conversion of Alkyl Halides and Alkyl Tosylates to Aldehydes. *J. Am. Chem. Soc.* **1959**, *81* (15), 4113–4114.

(40) Dave, P.; Byun, H.; Engel, R. An Improved Direct Oxidation of Alkyl-Halides to Aldehydes. *Synth. Commun.* **1986**, *16* (11), 1343–1346.

(41) Bratulescu, G. Synthesis of Aromatic Aldehydes by a Fast Method Involving Kornblum's Reaction. *Synth. Commun.* **2008**, *38* (16), 2748–2752.

(42) Mojr, V.; Herzig, V.; Budesinsky, M.; Cibulka, R.; Kraus, T. Flavin-Cyclodextrin Conjugates as Catalysts of Enantioselective Sulfoxidations with Hydrogen Peroxide in Aqueous Media. *Chem. Commun.* **2010**, *46* (40), 7599–7601.

(43) Chmurski, K.; Stepniak, P.; Jurczak, J. Improved Synthesis of C2 and C6 Monoderivatives of Alpha- and Beta-Cyclodextrin via the Click Chemistry Approach. *Synth.-Stuttg.* **2015**, *47* (13), 1838–1843.

(44) Wang, X. D.; Gu, X. S.; Yuan, C. W.; Chen, S. J.; Zhang, P. Y.; Zhang, T. Y.; Yao, J.; Chen, F.; Chen, G. Evaluation of Biocompatibility of Polypyrrole in Vitro and in Vivo. *J. Biomed. Mater. Res. A* **2004**, *68A* (3), 411–422.

(45) Yang, K.; Xu, H.; Cheng, L.; Sun, C.; Wang, J.; Liu, Z. In Vitro and In Vivo Near-Infrared Photothermal Therapy of Cancer Using Polypyrrole Organic Nanoparticles. *Adv. Mater.* **2012**, *24* (41), 5586–5592.

(46) Ateh, D. D.; Navsaria, H. A.; Vadgama, P. Polypyrrole-Based Conducting Polymers and Interactions with Biological Tissues. *J. R. Soc. Interface* **2006**, *3* (11), 741–752.

6.1. List of author's publications

1) Lukasek, J.; Boehm, S.; Dvorakova, H.; Eigner, V.; Lhotak, P. Regioselective Halogenation of Thiacalix[4]arenes in the Cone and 1,3-Alternate Conformations. *Org. Lett.* **2014**, *16* (19), 5100–5103.

2) Lukasek, J.; Strnadova, K.; Krabicova, I.; Rezanka, M.; Stibor, I. New Aligned Microfibers for Tissue Engineering. *Nanocon 2015: 7th International Conference on Nanomaterials - Research & Application* **2015**, 399–403.

3) Strnadová, K.; Lukášek, J.; Krabicová, I.; Stanislav, L.; Řezanka, M.; Jenčová, V.; Beranová, Š.; Stibor, I.; Lukáš, D. Functionalization and biocompatibility evaluation of drawn fibers for neural tissue implants. *Fiber Society 2016 Spring Conference: Textile Innovations - Opportunities and Challenges* **2016**, 126–127.

4) Lukášek, J.; Řezanková, M.; Stibor, I.; Řezanka, M. Synthesis of cyclodextrin–pyrrole conjugates possessing tuneable carbon linkers. *J Incl Phenom Macrocycl Chem* **2018**, *92* (3), 339–346.

5) Strnadová, K.; Stanislav, L.; Krabicová, I.; Sabol, F.; Lukášek, J.; Řezanka, M.; Lukáš, D.; Jenčová, V. Drawn aligned polymer microfibres for tissue engineering. *Journal of Industrial Textiles* **2019**, in press.

6) Lukášek, J.; Hauzerová, Š.; Havlíčková, K.; Strnadová, K.; Mašek, K.; Stuchlík, M.; Stibor, I.; Jenčová, V.; Řezanka, M. Cyclodextrin-Polypyrrole Coatings of Scaffolds for Tissue Engineering. *Polymers* **2019**, *11* (3), 459.